DYNAMIC SYSTEM REDUCTION AND FAULT LOCATION IDENTIFICATION USING SYNCHROPHASORS

by

EITHAR NASHAWATI

Presented to the Faculty of the Graduate School of

The University of Texas at Arlington in Partial Fulfillment

of the Requirements

for the Degree of

DOCTOR OF PHILOSOPHY

THE UNIVERSITY OF TEXAS AT ARLINGTON

May 2012

ACKNOWLEDGEMENTS

I am very thankful to my supervising professor Dr. Wei-Jen Lee for his support throughout my academic and professional career for a period of time that extended beyond the last decade. Dr. Lee supported me during my Master's and Ph.D. degrees and his great advice was sought for many of my career and personal decisions. Dr. Lee taught me qualities that are applied to not just my academic life, but to every aspect of my professional and personal life. Creativity, flexibility, and vision are great characters he promoted. I am also thankful to my supervising committee that provided constructive advice to my work. I extend my gratitude to Dr. William Dillon, Dr. Rasool Kenarangui, Dr. David Wetz and Dr. Sungyong Jung for their outstanding support.

I would also like to extend my greatest appreciation to my mother Inaam for her encouragement. To my wife Dana, I realize that you had to do more work than I did. To my daughters Maysa, Serene and Luna, I apologize for being busy sometimes, but I promise to make up as much time as possible.

Finally, I would like to remember and thank my late father Dr. Abdul Majid Nashawati for steering me in this direction. My promise to him has been fulfilled.

January 19, 2012

ABSTRACT

DYNAMIC SYSTEM REDUCTION AND FAULT LOCATION IDENTIFICATION USING SYNCHROPHASORS

Eithar Nashawati, PhD

The University of Texas at Arlington, 2012

Supervising Professor: Wei-Jen Lee

The advent of the synchronized phasor measurement units' technology allow for new applications to the power systems and improvement of existing applications. This dissertation presents a new method for synchrophasor-assisted fault location. An initial screening of voltage phase angle swing determines the suspect part of the system where the disturbance occurred. The system is then reduced to a limited number of buses. A Positive-sequence voltage-only method is then used to provide a better estimation of the exact location of the fault using particle swarm optimization. This method is applied to a large power system in North Texas. Real-time synchrophasor measurement units are used from across the power system to identify the fault location. Results are compared to traditional fault location methods that utilize non-synchronized current measurements to locate faults. Several cases are examined and results show accurate estimation of the fault location by using the proposed approach.

TABLE OF CONTENTS

LIST OF ILLUSTRATIONS

Figure Page

LIST OF TABLES

CHAPTER 1

INTRODUCTION

1.1 Introduction to Synchrophasors and Fault Location

"In 1893, Charles Proteus Steinmetz presented a paper on simplified mathematical description of the waveforms of alternating electricity. Steinmetz called his representation a phasor. With the invention of phasor measurement units (PMU) in 1988 by Dr. Arun G. Phadke and Dr. James S. Thorp at Virginia Tech, Steinmetz's technique of phasor calculation evolved into the calculation of real time phasor measurements that are synchronized to an absolute time reference provided by the Global Positioning System. Early prototypes of the PMU were built at Virginia Tech, and Macrodyne built the first PMU (model 1620) in 1992" [1].

The advances made in the synchronized phasor measurement unit (PMU) technology allow for new applications as well as improvements to existing applications. Digital relays provide an economical source of these measurements since many relay manufacturers include PMU capabilities in their relays. Synchronized measurements of the power system provide insightful data that was not visible prior to having PMU technology. The definition of a synchrophasor measurement is provided in IEEE Standard C37.118 and will be discussed in the next section.

New information is included in every PMU sampling data. In this dissertation, phase angle and magnitude of voltage measurements are used to screen PMU data and determine the locations of transmission system faults.

A transmission line short circuit event is the most common disturbance in the transmission network. The fault location problem is of a considerable significance because it expedites the restoration of the power system following faults. If the power system operator can

have an immediate estimation of the fault location, then direction can be given to field personnel to inspect the suspected area immediately and allow for swift restoration.

Several methods have been suggested for fault location. Most new distance microprocessor-based relays come with fault location capability. However, if such a relay is available on the faulted circuit, then data from that particular relay terminal will need to be extracted and may require trained personnel to examine it. Other methods require the knowledge of current quantities which then must be matched to the data of the short circuit model. This method also requires fault current monitoring on the faulted circuit. Chapter 2 will discuss the major fault location methods in more detail.

1.2 Synchrophasors Basics

Synchrophasors, or synchronized phasor measurements, provide means of referring the phasor representation of a power system voltage or current to an absolute time reference.

This absolute reference is provided in the form of a common timing signal by high-accuracy clocks synchronized to coordinated universal time (UTC) such as the universally used global positioning system (GPS) [2].

Many devices are capable of providing synchrophasor quantities. Most common devices are stand alone phasor measurement units (PMUs), numerical relays, and meters. The above mentioned devices shall have the capability to be connected to synchronized GPS clocks of high accuracy. The synchronized clock is used as a reference. Quantities that are recorded are analog sinusoidal quantities that have an instantaneous phase angle.

1.2.1 Definition of a Synchrophasor

IEEE standard C37.118 provides definition of a synchrophasor. The synchrophasor representation X of a signal x(t) is the complex value given by Equation (1):

$$X = X_r + jX_i$$

$$X = (X_m / 2)e^{j\varphi}$$

$$X = (X_m / 2)(\cos\varphi + j\sin\varphi) \tag{1.1}$$

The PMU device has the capability of recording a complex number (possible in rectangular or polar format) of the desired quantity represented by a specific timetag. The relationship between the reporting instant and the phasor representation is such that the phase angle of the phasor is equal to the angular separation between the reporting time and the peak of the sinusoid [2].

IEEE standard C37.118 dictates that as in Figure 1 first (solid) waveform, the peak of the signal coincides with the timetag yielding the angle measurement of 0, while in the second (dashed) waveform of Figure 1.1, the signal crosses zero at the timetag yielding a measurement of -90° [2].

The timetagged recorded quantity of a particular synchrophasor can be compared to other timetagged synchrophasor quantities of interest. This could lead to great enhancements in many power system applications. Recorded quantities can be any power system quantity available at the PMU device, such as voltage, current, frequency, active power and reactive power. In the case of numerical device that can process digital quantities, it is possible to record instances of digital assertion and de-assertion with respect to the high accuracy synchronized time signal.

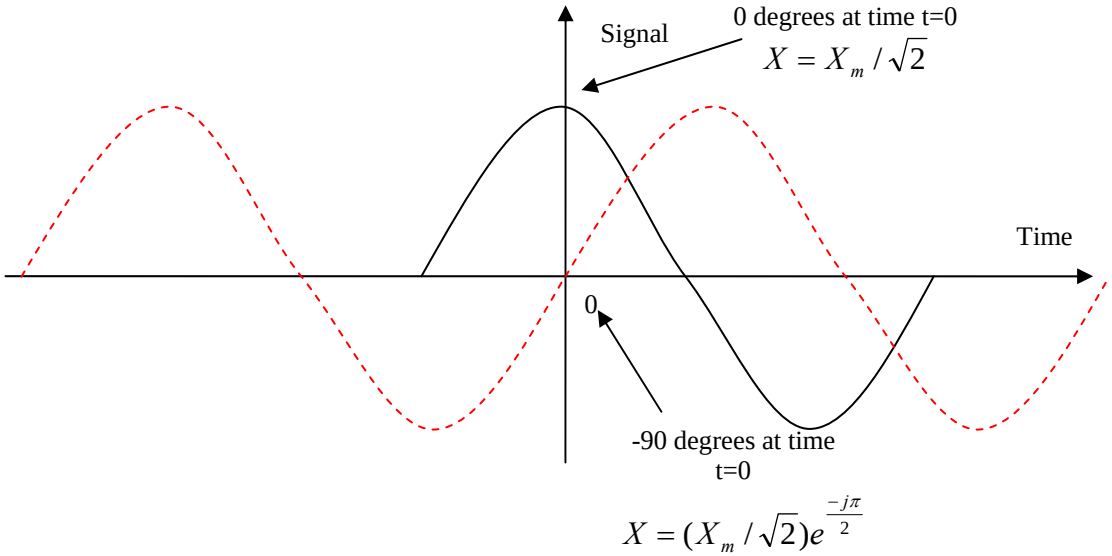

Figure 1.1 Convention for synchrophasor representation

Synchronized phasor measurements are becoming more popular. More utilities are installing PMUs on their systems. Many utilities are using synchrophasors for display or for post-event analysis. However, it is well recognized in the power engineering society that synchrophasors are going to play an increasingly significant role in the future in a wide variety of power system applications including wide area measurement networks, monitoring, control, event analysis, remedial action schemes, and system protection.

The location of the installed PMUs should be strategically selected to meet the goal of the utility. Cost is a major factor in deciding about the location of PMU locations. It is noticed that many newer numerical protective relays and meters have this capability built into their product, and this may be a cheaper way to get synchrophasor measurements. However, an adequate communication infrastructure must be in place to accommodate retrieval, transmittal, alignment and data concentration, processing, and backing-up of the synchrophasor data. As the amount of data retrieved continues to grow, high speed connections provide best option for

retrieval of synchrophasor data from different locations. However, special attention must be paid to cyber security threats and constraints.

1.3 The Fault Location Problem

Fault location is an important issue for power system operation. Finding the fault location following a fault allows for the quick restoration of the line which saves the utility company a significant amount of cost by reducing the number of resources needed to find the fault. Today's electric transmission systems are operated closer to their limits, and the loss of an element could exert extra burden on the grid which may result in a major system issue if coupled with other problems. Clear evidence of this is the Northeast blackout in 2003. Another reason for improving the fault location is minimizing the skill necessary to locate the fault. It could be time consuming to have a highly skilled person closely examine fault records to provide information to linemen. Automatic fault location methods that require no human intervention or judgment take precedence.

For the above reasons, researchers and power system engineers have invested lots of time and effort in trying to come up with fault locating methods that are simple, accurate, cost effective and dependable. This has been an interest area for engineers working for utility companies as well as protective relay manufacturers.

Both, traditional and newer methods for fault location are discussed in the next chapter. Most recently, researchers have made attempts to utilize synchronized phasor measurement units to locate faults and those will be discussed as well.

1.4 The Proposed Method

The use of synchronized phasor measurements have been suggested by researchers as in [4] and [5]. These methods were examined on small test cases and proven to be accurate. The basis for these methods is the bus impedance matrix. Calculations of the entire bus impedance matrix are not practical for large systems. Several methods exist for extracting certain columns and rows of the bus impedance matrix [6, 7]. However, large matrix operations are still necessary to achieve this extraction. Optimization methods are used to fit the fault

location parameters to measured parameters. This can also be mathematically challanging if complicated iteration methods are used.

The proposed method consists of three steps. Step one identifies the impacted area of a large power system based on phase angle measurement. Step two reduces the system to a small number of buses. Step three applies a positive sequence voltage method and particle swarm optimization to identify the fault location. In the proposed method, the phase angle swing method is used to reduce the studied area of the system to a small number of buses, and then the bus impedance matrix is calculated for the reduced system. Because of the reduction of the system, fault location search is preformed using a simple optimization method such as particle swarm optimization method.

1.5 Dissertation Outline

Chapter two provides background material on the fault location methods. First, a review of transmission line modeling is presented. Next, single-ended impedance based techniques are discussed. This discussion will include the simple reactance method and fault location methods with and without source impedance. Next, multi-ended, synchronized and unsynchronized data methods are discussed. Finally, other fault location techniques are also discussed and the discussion is extended to series compensated lines.

Chapter three is dedicated to providing background information on the optimization problem in general and the particle swarm optimization method in particular. Basic particle swarm optimization principles are presented.

Chapter four discusses the details of the new proposed method, including disturbance-area identification, system reduction using Gaussian elimination, fault parameter calculations, and applying the particle swarm optimization.

Chapter five discusses the application of the new method to a real power system in North and West Texas. Results of case studies from actual transmission line faults are discussed. The effect of source impedance changes is also considered.

Chapter six concludes the dissertation. It includes concluding remarks, a highlight of the dissertation contribution and future work.

CHAPTER 2

FAULT LOCATION METHODS

2.1 Review of Transmission Line Modeling

This chapter provides a quick review of the transmission line modeling basics. Generally, many power systems books discuss classifications of transmission line lengths. Overall [6],

- A long line is a line of length $\ell > 150$ miles.
- Medium length lines are lines with $50 > \ell > 150$ miles.
- Short length lines are lines with $\ell < 50$ miles.

The following terms will be used,

$z = r + jwl$ is the line impedance per unit distance (meter)

$y = g + jwc$ is the line shut admittance (to neutral) per unit distance (meter)

$Z = z\ell$ is the total line impedance

$Y = y / \ell$ is the total line shunt admittance to ground

Where ℓ is the total line length

$\gamma = \sqrt{yz} = jw\sqrt{lc} = \alpha + j\beta$ is called the propagation constant

$Z_C = \sqrt{\frac{Z}{C}}$ is the characteristic impedance of the transmission line

Next we define the π-equivalent circuit model as shown in Figure 2.1, where

$$V_S = AV_R + BI_R \tag{2.1}$$

$$I_S = CV_R + DI_R \tag{2.2}$$

Which can be shown as,

$$\begin{bmatrix} V_S \\ I_S \end{bmatrix} = \begin{bmatrix} A & B \\ C & D \end{bmatrix} \begin{bmatrix} V_R \\ I_R \end{bmatrix} \tag{2.3}$$

where

V_S is the sending-end voltage,

I_S is the sending-end current,

V_R is the receiving-end voltage, and

I_R is the receiving end current,

$$A = 1 + \frac{Z'Y'}{2}$$

$$B = Z'$$

$$C = Y'\left(1 + \frac{Z'Y'}{4}\right)$$

$$D = 1 + \frac{Z'Y'}{2}$$

$$Z' = Z\frac{\sinh \gamma\ell}{\gamma\ell}$$

$$\frac{Y'}{2} = \frac{Y}{2}\frac{\tanh(\gamma\ell/2)}{\gamma\ell/2}$$

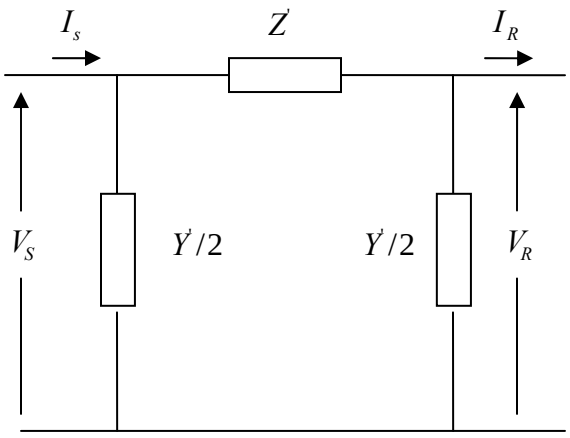

Figure 2.1 The π-equivalent circuit model of a transmission line

2.1.1 Short Lines

This is the simplest model where all line shunt admittance to neutral is ignored in the model. This results in the following relationships,

$$V_S = V_R + ZI_R \tag{2.4}$$

$$I_S = I_R \tag{2.5}$$

It was assumed here that $Z' = Z$. This assumption is accepted here because $\frac{\sinh \gamma\ell}{\gamma\ell} = 1$.

2.1.2 Medium-Length Lines

In medium-length lines, the shunt admittance becomes considerable. The model used is generally the π-equivalent circuit model but still making the assumptions that $Z' = Z$ and $Y' = Y$. This is because

$\frac{\sinh \gamma\ell}{\gamma\ell} = 1$, and

$\frac{\tanh(\gamma\ell/2)}{\gamma\ell/2} = 1$

We obtain the following relationship equations,

$$V_S = (1 + \frac{ZY}{2})V_R + ZI_R \tag{2.6}$$

$$I_S = Y(1 + \frac{ZY}{4})V_R + (1 + \frac{ZY}{2})I_R \tag{2.7}$$

2.1.3 Long Lines

To create a simplified model of a long transmission line, the π-equivalent circuit model is used but without any simplifications like those made for the medium-length lines. The relationship equations are

$$V_S = (1 + \frac{Z'Y'}{2})V_R + Z'I_R \tag{2.8}$$

$$I_S = Y'(1 + \frac{Z'Y'}{4})V_R + (1 + \frac{Z'Y'}{2})I_R \tag{2.9}$$

For voltage dependent fault location methods, the appropriate line model shall be used. It is noticed that in the case of short transmission lines, the voltages are only dependent on the line series impedance. However, for medium-length and long transmission lines, the effect of the shunt admittance becomes greater and can result in voltage errors if not modeled correctly.

2.2 Fault Location Overview

The fault location problem is an old problem. A short circuit event is the most common disturbance on the transmission grid. Faults can be phase-to-ground (most common type), phase-to-phase, phase-to-phase-to-ground, three-phase or three-phase-to-ground. A three-phase fault is the rarest type of fault. Protection Engineers have been researching this area for a long time. Operationally, accurate estimation of the fault location is very valuable. The main motivation for improving fault location techniques is the quick restoration of the faulted transmission line (in the case of a line lockout), or finding the fault to be able to perform maintenance before a temporary fault would come back as permanent fault during a bad time. Another reason is the savings resulting from less line inspections. Moreover, finding faults,

even temporary ones, aids in verifying and correcting the short-circuit model used by the utility company.

Different techniques for fault location are discussed in this chapter. This discussion will include “impedance-based” fault location techniques. Several algorithms have been developed under this category. Most algorithms utilize single or dual-ended voltage and current quantities to locate faults. Single-ended algorithms have been widely examined. These are simple methods. Typical challenges are fault resistance, load and other simplification assumptions. If source impedance is used, then it is subject to changes due to the power system changes. Dual-ended methods do not require knowledge of the system outside of the faulted line, and usually include no simplifying assumptions. However, typical challenges to this type of method are communication to both ends of the line, and minimizing or eliminating effects of some factors such as fault resistance, current distribution factors and load. Other techniques include synchronized or non-synchronized phasor measurements algorithms.

In the recent years, utilities have started installing PMU measurements across their systems. However, most utilities still have very few synchrophasor points installed, which limits the application development to take advantage of these installations. Different utilities are recording different quantities and at different sampling rates. Most utilities record voltages but may not record currents. They may record only positive sequence quantities. Since applying PMU information for fault location is still in its beginning stage, voltage-only methods are described in this chapter as well.

2.3 Single-Ended Fault Location Schemes

Single-ended fault location algorithms are desirable because they do not require communication links between the ends of the faulted line. Only local quantities are utilized in such methods. This makes single-ended methods attractive for application in protective relays and single-ended fault locaters. The need for only one device on the local end makes these methods less costly.

Single-ended fault location schemes are generally impedance based schemes. These types of schemes require the measurement of voltage (phase to ground) and current of each phase from one end of the faulted circuit to calculate the apparent impedance from that terminal. This type of scheme is widely available in most modern numerical distance protective relays. These methods typically require fault type identification prior to applying the different algorithms of fault location. If the fault resistance is assumed to be zero, we can use one of the impedance calculations in Table 2.1 to estimate the fault location [15].

Table 2.1 Simple Impedance equations

Fault Type	Positive Sequence Impedance Equation mZ_{1L}
A-ground	$\frac{V_a}{I_a + k3I_0}$
B-ground	$\frac{V_b}{I_b + k3I_0}$
C-ground	$\frac{V_c}{I_c + k3I_0}$
a-b or a-b-g	$\frac{V_{ab}}{I_{ab}}$
b-c or b-c-g	$\frac{V_{bc}}{I_{bc}}$
c-a or c-a-g	$\frac{V_{ca}}{I_{ca}}$
a-b-c	$\frac{V_{ab}}{I_{ab}}$ or $\frac{V_{bc}}{I_{bc}}$ or $\frac{V_{ca}}{I_{ca}}$

Where,

$k = \frac{Z_{0L} - Z_{1L}}{3Z_{1L}}$,

Z_{0L} is the zero-sequence line impedance,

Z_{1L} is the positive-sequence line impedance (it is reasonable to assume that positive-sequence line impedance is the same as negative-sequence line impedance),

m is the per unit distance to fault (for example: distance to fault in kilometers divided by the total line length in kilometers), and

I_0 is the zero-sequence current.

Figure 2.2 shows the one-line circuit and representation of a line fault [8, 15].

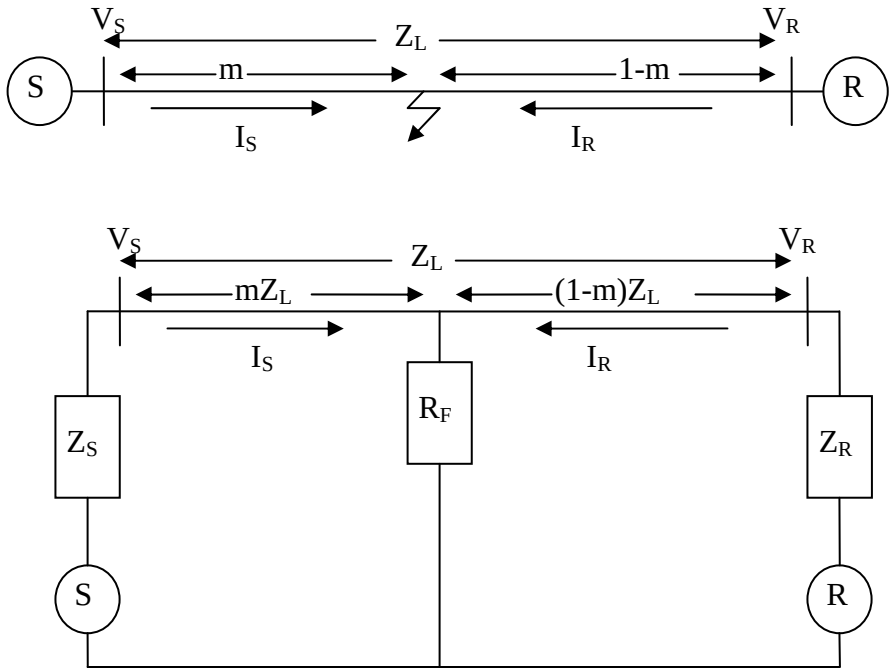

Figure 2.2 One-line and circuit representation of a line fault

Note that to use the equations in Table 2.1, the fault type must be identified. There are several sources for error when using the above simplistic approach. Errors are a result of assumptions and simplifications, or incorrect data. Some of these error sources are as follows:

- Pre-fault Load current, and unbalance in the load current.
- Fault resistance, which can be high especially on distribution circuits.
- Wrong type of fault is identified.
- Mutual coupling, especially zero sequence mutual coupling for faults involving ground.
- Model errors.
- Instrument transformer errors.

Next section discusses several methods that were developed to eliminate or reduce some of these errors.

2.3.1 Simple Reactance Method

In the system shown in Figure 2.1, the following assumptions are made

- The line between S and R is homogenous. IEEE standard C37.114 defines a homogenous line as a transmission line where impedance is distributed uniformly on the whole length.
- Z_R and Z_S are the Thevenin equivalents of the system at the remote terminals (source impedances.)
- The fault has fault resistance R_F. I_F is the fault current.
- Z_L is the line impedance

V_S, the voltage at bus S, can be calculated as

$$V_S = mZ_L I_S + I_F R_F \tag{2.10}$$

If we divide both sides of (2.10) by I_S, then the above equation becomes

$$V_S / I_S = Z_{FS} = mZ_L + (I_F / I_S) R_F \tag{2.11}$$

Z_{FS} is the apparent impedance at bus S. The simple reactance method, as the name implies, is only concerned with the imaginary part of the above equation. Therefore, the second term $(I_F / I_S)R_F$ is assumed to be a real number or zero. This is equivalent to assuming that I_F and I_S are in phase, $I_R = 0$, or $R_F = 0$. The imaginary part (reactance part) of the above equation becomes mX_L. This yields the following distance to the fault.

$$m = \frac{\mathrm{Im}(V_S / I_S)}{X_L} \tag{2.12}$$

The value or the positive-sequence impedance in the numerator is readily available in Table 2.1 for the different types of faults. Different methods and algorithms used in determining the fault type play a very important role in this method. An error in the fault type identification leads to the incorrect estimation of the fault distance.

The lack of tolerance of the algorithm to fault resistance made it less attractive. Because the above method involved assumptions that can not always be met, there is a need for another method that eliminates the need for making these kind of assumptions.

2.3.2 One-Ended Method without Source Impedance

This method is commonly referred to as the Takagi method. This method was described by T. Takagi with Tokyo Electric Power in 1982. Since then, many researchers have used it as a basis for one-ended fault location methods that do not utilize source impedance. Previously, we determined that

$$V_S / I_S = Z_{FS} = mZ_L + (I_F / I_S)R_F$$

If I_F and I_S are not in phase, then $(I_F / I_S)R_F$ is a complex number. This could cause errors in any reactance based fault location method.

The Takagi method separates a single phase circuit with a fault into two circuits, a load flow component circuit and a fault component circuit. The load flow component is the pre-fault

circuit. Figure 2.3 shows these equivalent circuits [9]. This figure is the breakdown of the S-source side of Figure 2.2.

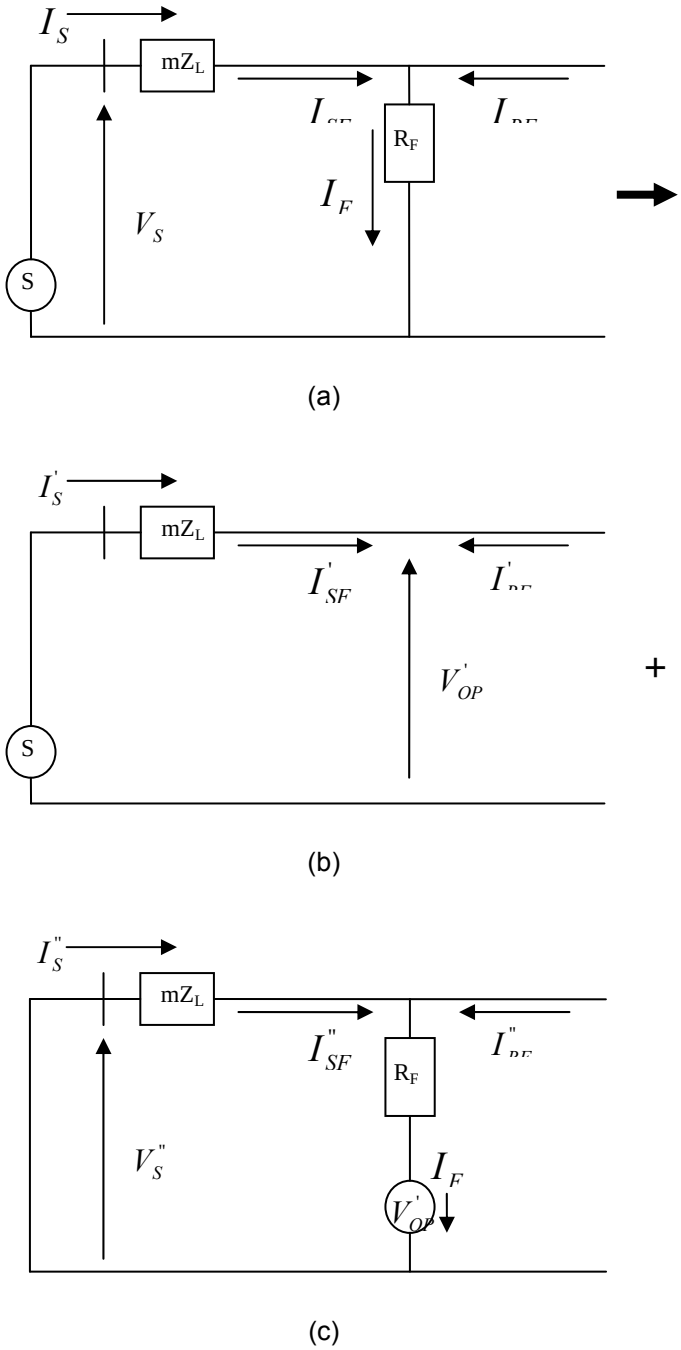

Figure 2.3 The Takagi breakdown of a fault circuit. (a) The single-phase circuit with a fault, (b) The load flow component and (c) The fault component

Where,

I_{SF} is the fault-point current from S terminal

I_{RF} is the fault-point current from R terminal

$V_S^{"}$ is the voltage difference between pre-fault and after-fault voltage

$I_S^{"}$ is the current difference between pre-fault and after-fault (fault component current)

$I_{SF}^{"}$ is the fault current from S terminal

$I_{RF}^{"}$ is the fault current from R terminal

The voltage at bus S, can be calculated as in (2.10)

$$V_S = mZ_L I_S + I_F R_F$$

If we multiply both sides by the conjugate of $I_S^{"}$, then we get:

$$V_S I_S^{"*} = mZ_L I_S I_S^{"*} + I_F R_F I_S^{"*} \quad (2.13)$$

Considering the imaginary part only of the above equation

$$\mathrm{Im}(V_S I_S^{"*}) = m.\mathrm{Im}(Z_L I_S I_S^{"*}) + R_F\ \mathrm{Im}(I_F I_S^{"*}) \quad (2.14)$$

Solving for the distance m we get

$$m = \frac{\mathrm{Im}(V_S I_S^{"*})}{\mathrm{Im}(Z_L I_S I_S^{"*})} \quad (2.15)$$

The above is completely accurate if the term $R_F\ \mathrm{Im}(I_F I_S^{"*})$ has no imaginary part. This is true if the fault component current from S terminal and the fault-point current are in phase. By using the fault component current or “difference” current, the load current effect is eliminated. The fault component current from S terminal and the fault-point current are in phase if the system is homogenous. IEEE standard C37.114 defines a homogenous system as a transmission system where the local and remote source impedances have the same system angle as the line impedance.

Takagi suggested a modified equation that compensates for contribution of other phases in the same line or phases of other mutually coupled lines. The compensation is as follows (equations shown are for one line, but apply to both lines in the case of mutually coupled lines)

For an A phase to ground fault

$$m = \frac{\mathrm{Im}(V_A I''^{*}_{\alpha A})}{\mathrm{Im}(V_{LA} I''^{*}_{\alpha A})} \tag{2.16}$$

Where,

V_A is the line A phase voltage

$I''^{*}_{\alpha A}$ is the α component of the line A phase current (fault component)

$V_{LA} = \sum_K (Z_{AK} I_K)$, K = A, B, C for both mutually coupled lines

Z_{AK} is the mutual impedance of A phase and phase K for K=A, B, C

The above equation can be applied to any phase of the three phases of either line.

For an A-B phase-to-phase fault (also includes phase-to-phase-to-ground fault and three-phase faults)

$$m = \frac{\mathrm{Im}(V_{AB} I''^{*}_{AB})}{\mathrm{Im}(V_{LAB} I''^{*}_{AB})} \tag{2.17}$$

Where,

V_{AB} is the A-B phase-to-phase voltage

I''^{*}_{AB} is the A-B phase-to-phase current (fault component)

$$V_{LAB} = (Z_{AA} - Z_{AB}) I_A - (Z_{BB} - Z_{AB}) I_B + (Z_{CA} - Z_{CB}) I_C + \sum_K (Z_{AK} - Z_{BK}) I_K \tag{2.18}$$

K = A, B, C for the un-faulted mutually coupled line only.

A simplification Takagi made in deriving $m = \frac{\mathrm{Im}(V_S I_S^{"*})}{\mathrm{Im}(Z_L I_S I_S^{"*})}$ is

$$\tanh(\gamma m) = \gamma m$$

Where γ is the propagation constant of the transmission line.

The above simplification is a commonly made assumption for short lines. This simplification is used in lumped-circuit equivalents.

Takagi compensated for this approximation error as well. If m_{new} is the compensated fault location, and m is the non-compensated then

$$m_{new} = m - (\beta^2 m^3 / 3) \tag{2.19}$$

Where,

β is the imaginary part of the propagation constant γ. Details of how this compensation factor is derived are discussed in reference [9]. Another error source in this method is the effect of the fault current in the overhead ground wire.

A modified Takagi method is mentioned in [8, 15]. This method substitutes the zero-sequence current in place of the fault component current. This eliminates the need to know the load flow data. This is done for ground faults. A correction angle can also be added to improve the accuracy. This angle is the angle difference between the ground current from the end where fault location is done and the fault current. This makes the algorithm accurate for only one location on the line, which is the fault location assumed in finding this angle.

Next, single-ended fault location algorithms with remote source impedance settings will be discussed. However, it is advantageous to locate faults from single-end quantities without the source impedance setting, as this value is subject to change as the system operating conditions change.

2.3.3 One-Ended Method with Source Impedance

As discussed previously, single-ended fault location algorithms that do not utilize source impedance can create considerable error if the current infeed from the remote end is significant and the fault impedance cannot be ignored. This infeed current creates a difference in the magnitude and angle between the fault current and the current at the local end where the fault location algorithm is applied. This is also a variable based on the fault location on the line. Compensating for this angle error can give improved results but for only one location on the line, which is the location assumed in finding angle.

A method that utilizes source impedance at both ends of the transmission line is discussed in reference [10]. Going back to Figures 2.2 and 2.3(c), we can realize the following relationship

$$I_S^{"} / I_F = \frac{(1-m)Z_L + Z_R}{Z_S + Z_L + Z_R} \tag{2.20}$$

The ratio of $I_S^{"} / I_F$ is defined as the fault distribution factor D_s.

$$D_s = I_S^{"} / I_F$$

This factor is used in the subsequent discussion. Using symmetrical components, we can extract the following relationships for a phase-to-ground fault

$I_F = 3I^0$ and $I^+ = I^- = I^0$

Where,

I^+ is the positive-sequence current

I^- is the negative-sequence current

I^0 is the zero-sequence current

We have also realized previously in (2.10) that

$$V_S = mZ_L I_S + I_F R_F$$

We can obtain equation (2.20) by substituting the fault current from the distribution factor relationship

$$V_S = mZ_L I_S + (I_S^{"} / D_s)R_F \tag{2.21}$$

Substituting the distribution factor D_s with its value obtained earlier we get the following equation

$$m^2 - (\frac{V_S}{I_S Z_L} + \frac{Z_R}{Z_L} + 1)m + (\frac{Z_R}{Z_L} + 1)\frac{V_S}{I_S Z_L} - R_F \frac{I_S^{"}}{I_S Z_L}(\frac{Z_S + Z_R}{Z_L} + 1) = 0 \tag{2.22}$$

The above equation has a real part and an imaginary part that equal zero. R_F and m are the two unknown variables, therefore it is possible to solve for m. Reference [10] provided a modification of the above equation for mutually coupled lines as well.

The above method requires the knowledge of the source impedances on both ends of the faulted transmission line. This is a required setting in the device to perform this algorithm. The problem here is that if this setting is not accurate, then this method will produce errors. System configurations and operating conditions can change and affect the source impedance settings.

2.4 Multi-Ended Fault Location Schemes

Most methods suggested by researchers in this category are for two-terminal transmission lines. A few researchers have looked into three-terminal transmission line fault location, but more analyses need to be performed. The vast majority of transmission lines are two-terminal lines, and therefore the following discussion provides some background about the two-ended fault location methods.

Single-ended fault location methods discussed previously have deficiencies due to uncertainties of fault resistance, load, and angle mismatch of infeed currents resulting in fault voltage angle mismatch between the end where the fault is located and the fault location.

As communication technologies advanced, it became possible to get fault measurements from both ends of the faulted transmission line. This includes voltage and

current. In Figure 2.2, using quantities from both ends of the line, the fault point voltage can be easily described by forming two equations for voltage loops, one from each end of the line, as follows.

$$V_f = V_S - mZ_L I_S \tag{2.23}$$

$$V_f = V_R - (1-m)Z_L I_R \tag{2.24}$$

(2.23) and (2.24) are solved simultaneously to find the fault location m .

$$m = \frac{((V_S - V_R)/Z_L) + I_R}{I_S + I_R} \tag{2.25}$$

Some of the benefits of the using the above fundamental technique are

- Simplicity.
- Insensitivity to the external system (source impedances are not needed).
- Insensitivity to load flow.
- Unaffected by the fault resistance.
- Fault type identification is not needed.

By using the positive-sequence or negative-sequence quantities in the above equation, the need for fault type identification is eliminated. This improves the accuracy of these methods as the zero-sequence component can introduce errors due to uncertainty of the zero-sequence network. These uncertainties stem from unbalanced loading and mutual coupling. Another benefit of not needing fault type identification is the possible poor performance of fault type identification methods for evolving faults. Evolving faults are those that start as one type, but change into another type of fault. For example, a fault may start as a phase-to-ground fault and become a three-phase-to-ground fault. Depending on the algorithm and the instance in the fault record the fault type identification is applied, the fault locator may deem the wrong fault type, and therefore, use the wrong quantities to derive the fault location. Examples of fault location errors because of this phenomenon are provided in technical papers [8].

However, m is not the only unknown in the above fault location equation. If the voltage and current measurements from both ends are not synchronized, then it will not be possible to apply the fault location equation above. Therefore, several methods developed by researchers [11-12, 47] have attempted to solve the above equation using different techniques that would all try to identify the angle difference between both end quantities because of the non-synchronization. In this case, the fault location from two ends can be done off line, unless a communication link is available and it is not costly to implement it on line.

It is worthwhile to note that the methods that use non-synchronized measurement at both ends of the transmission line can be applied to synchronized measurement methods. However, the opposite is not true. Non-synchronized methods may be applied even on synchronized measurement to improve accuracy and solve other issues such as sampling rates and phase shifts introduced in different recording devices and transducers [47].

Reference [12] derives the equations for the apparent impedance at each end of the line Z_S and Z_R as seen by the fault locator and creates one equation by adding the two equations. Next, the relative angle between the two end currents is found $\frac{I_R}{I_S} = p\angle\theta$, and then the relative angle between the two end voltages is found using,

$$V_S = Z_S I_S \tag{2.26}$$

$$V_R = Z_R I_R \tag{2.27}$$

Only relative angles are needed in all algorithms of such nature, because one end can be used as reference (having 0 degrees angle at the instance of the fault location calculation, and the other end will have the relative angle as phase angle for the same instance).

Reference [47] solves the same problem by using an iterative approach to obtain a synchronization angle. It is assumed in this method that

$$V_S = V_S\angle(\alpha_m + \delta) \tag{2.28}$$

$$V_R = V_R \angle(\beta_m) \tag{2.29}$$

Where,

α_m and β_m are the measured angles, and

δ is the angle required to synchronize the phasors at bus S to those at bus R.

The above quantities are substituted in the main fault location equation (2.25) obtained earlier and substituting

$\delta = e^{j\delta} = \cos(\delta) + j\sin(\delta)$ and

$Z_L = R_L + jX_L$

Then, the equation is separated into real and imaginary parts, resulting in the following equation

$$a\sin(\delta) + b\cos(\delta) + c = 0 \tag{2.30}$$

Where a, b and c are constants given in reference [47]. The only unknown in the above equation is δ. The author of this paper then selects the Newton-Raphson method to determine δ. Newton-Raphson method is widely used in the power system application such as power flow solutions. It uses a function, its derivative, and an initial guess to determine the value of a variable.

$$x_{n+1} = x_n + \frac{f(x_n)}{f'(x_n)} \tag{2.31}$$

For this case the function is the equation found above, and its derivative can be easily found.

Reference [47] suggests an initial guess of $\delta_0 = 0$. This choice is realistic because in practical power systems, this angle has a limited range. After this angle is determined, the fault location equation can easily be solved. Because of the problems associated with the zero-sequence network described earlier, the authors recommend the use of positive-sequence or negative-sequence quantities. The authors also point out that negative sequence maybe more

accurate because of pre-fault negative sequence quantities are relatively small and can be ignored. However, it is noted that for three phase balanced faults, the negative sequence component does not exist. A hybrid method that uses negative-sequence for unbalanced faults and positive-sequence for balanced faults can be used, but will require fault type identification. As mentioned earlier, fault type identification could bring its own set of problems. Therefore, positive-sequence is the method of choice for applying the above algorithm. This reference also provided compensation factors for long lines where shunt admittance can not be ignored and a π-equivalent circuit model shall be used. It was mentioned that this method was tested using staged faults on 500kV transmission lines and proved accurate.

Another method for determining the distance to the fault is suggested in reference [45]. In this method, the author suggests an algorithm that utilizes three phase quantities to solve for the fault location. For two-end three-phase voltage and current synchronized measurements, the authors use the two main voltage equations (2.23) and (2.24) and subtract one from another to get an equation with one unknown (distance to the fault). The algorithm then utilizes the least-squares to find the distance to the fault. For non-synchronized measurements, the algorithm assumes one end as a reference (voltage equation unchanged), and inserts an angle (synchronization angle) in the voltage drop equation of the second end. The algorithm uses an iterative solution with least square method to solve for two unknowns (fault location and synchronization angle). Initial estimates of the fault location can be 50% or 0% and an initial value of the angle of 0 degrees is used. The method is also extended to three-terminal lines with and without synchronization. The author reported excellent results for a variety of faults on test cases using steady state short circuit program and electromagnetic transient program.

2.5 Other Fault Location Schemes

2.5.1 Voltage-Only Methods

Reference [5] reports a new method based on the bus impedance matrix. The fault location is assumed to be a new bus inserted into the existing bus impedance network. The author derives equations and parameters to modify the bus impedance matrix in terms of the

location of the fault. This method allows for direct modification of the bus impedance matrix. Following the modification, basic three-phase analysis of the fault is performed. Three phase, positive, negative and zero-sequence component fault voltages are calculated. Positive, negative and zero-sequence component fault currents are also calculated in terms of the sequence voltages and the modified bus impedance matrix. The author then describes algorithms for locating faults using voltage magnitude from one bus. This is done by using the least squares method to solve the three phase voltage equations and the fault current equation for the unknowns of fault resistance and fault location. The drawback of this method is the need to identify the fault type so that the correct set of equations can be applied. Other error sources are the estimation of small fault resistance for three phase faults, and assuming of 1 p.u. pre-fault voltage. The author also suggested a method that uses multiple voltage measurements but still requires fault location identification and makes assumptions about pre-fault voltages. However, it does not require any assumptions about the fault resistance for three phase faults. Least squares method is also used.

Reference [13] suggests the use of synchronized phasor measurements from two buses to obtain the distance to the fault based on a modified bus impedance matrix as described in the previous paragraph. In reality, you have to know the faulted branch and this method can produce several candidates with the matching results for a large-size power system.

2.5.2 Traveling-Wave Methods

Traveling wave methods have been in use for a long time. The main concept of these methods is to capture the surges (or traveling waves) on the transmission line following a fault. This is a high frequency wave. Capturing can be done using current transformers or voltage transformers. Recently, coupling capacitor voltage transformers (CCVTs) had become widely used by utilities. The winding of the CCVTs may prevent the unit from reproducing these transients on the secondary windings of the CCVT. Additionally, the stronger the bus, the lower the surge voltages are. Therefore, current transients may be more appropriate for the purpose

of fault location. Sensors are used to capture the surge pulses. When the pulses are captured, the distance to the fault can be calculated with the information regarding the speed of traveling wave. It must be noted that very accurate time referencing shall be used. Current GPS clock technology is accurate up to one microsecond. If the speed of traveling wave is $3x10^5$ kM/sec, the above clock accuracy translates into 152.4 m.

Traveling wave methods are also divided into single-ended and two-ended methods. Single-ended methods rely on the surge created by the fault, and the reflection again from the same fault after it reaches the recording end of the transmission line. This method measures the time between the consecutive captured surges and calculates the distance to the fault based on the time difference. A problem could arise if the fault is not capable of reflecting the wave back due to the arc extinguishing. Single-ended methods can be degraded by reflections from other sources such as tapped load, stations, or line taps.

Two-ended fault location methods are more accurate. This is due to insensitivity to reflection sources mentioned above. Two-ended methods capture the first wave initiated by the fault at both ends of the transmission line. Using the data from both ends, it is fairly simple to calculate the distance to the fault. However, similar to other fault location methods discussed earlier in this dissertation, the two-ended fault location methods require twice the hardware needed for a single ended method. Although the fault location analysis does not need to be run online, a communication link still needs to exist to obtain the recorded data from both ends of the transmission line. All traveling wave methods require high accuracy clocks and usually special fault location equipment capable of detecting the leading edges of the high frequency surges.

2.5.3 Series-Compensated Lines

Power transfer over long transmission lines is limited by the reactive impedance of the line [14]. Series compensation is an old but effective method to cancel some of the impedance of the line and make the line appear shorter. This increases the amount of transferrable real power on the line.

Series capacitor bank can be installed anywhere on the transmission line and usually do not exceed 70% compensation. This means that the capacitive reactance of the series capacitor bank does not cancel out more that 70% of the inductance of the line. The installation can be at either end of the line, in the middle of the line, or even have more than one series capacitor bank in one line (divided up).

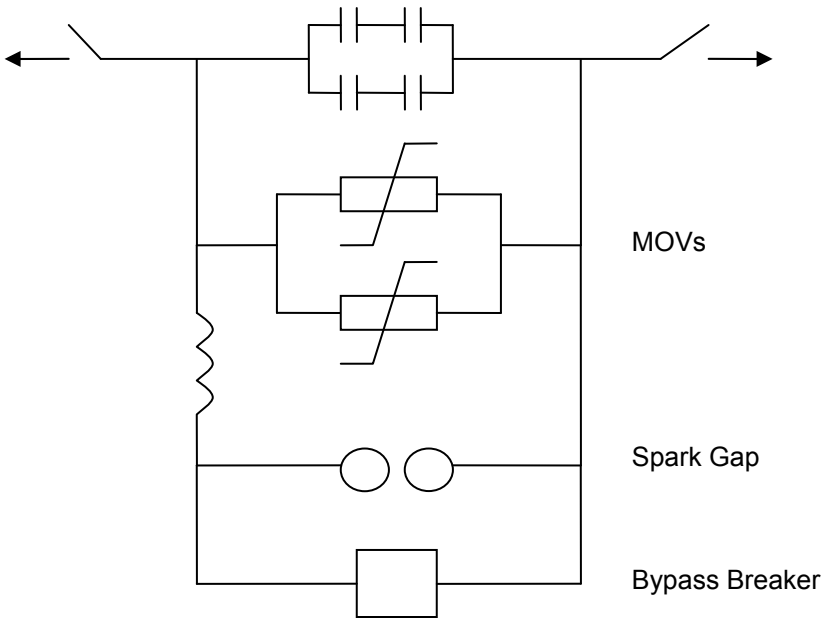

Figure 2.4 Single line diagram of a series capacitor protected by MOVs and a triggered gap

During transmission line faults, high fault current will pass through the capacitors. The impedance of the capacitor will cause a voltage to be developed across the capacitor. The capacitor needs to be protected against this overvoltage. As shown in Figure 2.4, traditionally the series capacitor is protected by a spark gap. Common designs now include metal oxide varistor (MOV) in parallel with the capacitors. The series compensation installation is designed to a specific protective level current. The protective level current determines the peak voltage developed at the capacitor for a certain rated bank current. Typical protective level current is 2 to 2.5 times of the rated current.

The MOVs are responsible for limiting the voltage developed across the capacitors to the design limits (protective level). The MOVs absorb large amount of energy, and the compensation controller typically receives current measurements from current transformers in the MOV branches. The controller also receives temperature information, and can therefore determine the energy that is being absorbed by the MOVs. At a certain threshold, the controller will send a signal to the triggered-gap to operate and bypass the capacitor. A bypass breaker closes to bypass the whole series compensation installation a few cycles later.

When the series compensation capacitor bank is at the station end, then the voltage measuring device (potential transformer or coupling capacitor voltage transformer) can be located at the line side of the series capacitor to overcome the voltage problem. However, when the series compensation capacitor bank is located in the middle of the line, and the fault occurs between the capacitor bank and the other end of the line, then the local end fault locator will be impacted by the voltage drop on the capacitor, which is commonly referred to as voltage reversal. This will cause erroneous results for impedance based fault location algorithms.

From the previous discussion, it is obvious that the impedance of the transmission line is not constant. When the series capacitor bank is in service, then the impedance of the line is at a certain value. When the MOVs start to conduct, then the impedance starts to change. The MOV is a nonlinear impedance device. Finally, when the spark gap fires, the capacitor bank is completely removed from the line. Therefore, the impedance changes with time. This means that the voltage drop across the capacitor bank is also difficult to calculate. This makes fault location very complicated.

An additional complication with capacitor banks is the appearance of non-fundamental frequencies current. This includes a low frequency and high frequency components. The low frequency is caused by resonant circuit between the capacitor bank and the inductance of the line. Usually, this is an oscillation that will damp out with time, but not during normal fault clearing time for a high voltage transmission line [15]. The high frequency transients are

caused by the operation of the triggered gap. Adequate filtering techniques in modern numerical devices can effectively remove these components [16].

Most methods that try to locate faults using impedance methods will have to compensate for the above discussed voltage drop. To accomplish this, these methods involve creating a model for the series capacitor. Reference [17] suggests a linear model to represent the series capacitor bank. This model replaces the capacitor and the parallel MOVs by series impedance as shown in Figure 2.4.

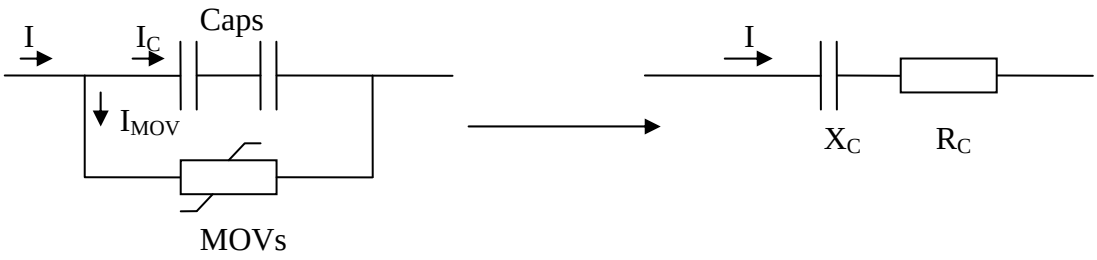

Figure 2.5 The linear model of the capacitor bank and MOVs

The basis for the above linear model is the observation made in the modeling Goldsworthy performed as discussed in Reference [17]. The main observation that led to the above model was made after modeling a series capacitor bank in the Electromagnetic Transients Program (EMTP). It is established that the fault current is sinusoidal. However, the MOVs' current is not sinusoidal since it conducts during each half cycle. Goldsworthy noticed that the combination current is still largely sinusoidal. By performing EMTP simulations, Goldsworthy was able to find a relationship between fault current and the capacitor-MOVs equivalent. The following results are reported

$$R_C = X_{CAP}(0.0745 + 0.49e^{-0.234I_{PU}} - 35e^{-5I_{PU}} - 0.6e^{-1.4I_{PU}}) \quad (2.32)$$

$$X_C = X_{CAP}(0.1010 + 0.005749I_{PU} + 2.088e^{-0.8566I_{PU}}) \quad (2.33)$$

Where,

$I_{PU} = \frac{I}{I_{PR}}$, I_{PR} is the protective level current, and

X_{CAP} is the series capacitor bank reactance.

It should be noticed that the above equations are only accurate for $I_{PU} > 0.98$. Below 0.98, the MOVs are assumed to be not conducting.

From the above equations, it is noticed that the equivalent model is a function of the protective current level and the reactance of the series capacitor bank. This model assists with calculating fault current that is not exact, but is a good approximation. The method first calculates fault current without the MOVs. Then it uses the above equations to calculate the equivalent. The equivalent is then used to update the model and calculate a new fault current, which is used to calculate updated values of the equivalent and so forth. The above iteration continues until good convergence occurs. Goldsworthy reposts that a maximum number of nine iterations have been needed. He also reports that the model results have been compared to staged faults and proven to be good. This method is used in new short-circuit programs such as ASPEN to find the fault current for a series capacitor installation. The method is simple, and requires very little information about the series capacitor. Only the protective level current and per unit compensation (impedance values) are needed.

The above linear model has been used in fault location algorithms such as the one suggested in reference [18]. This method uses single-ended data, and the Goldsworthy model to create fault location algorithms that calculates fault locations in front and behind the series capacitor location. Next, a selection is made whether the fault is in front of or behind the series capacitor. The selection issue can be treated as a separate issue.

The above review of series compensated lines is necessary to complete the discussion later about the proposed new fault location method.

An alternate method to locate faults on transmission lines is the use of traveling wave methods. Traveling waves are insensitive to series capacitor installation, and therefore can be a great alternative to traditional or capacitor-MOVs model methods.

CHAPTER 3

OPTIMIZATION METHODS

3.1 Review of Optimization Methods

Optimization methods are used to search a space for an optimum solution. The solution may be subject to certain various constraints (linear or non linear). The solution may have multiple candidates. Also, there maybe more than one quantity to be optimized (multiple object functions).

The power system is no exception to the above. It is designed and operated with different constraints. It has a large number of components, configurations, operating conditions, and is changing with time. Reference [19] lists four criteria to select an optimization method that best fits a certain problem. The optimization method must

- Match the problem.
- Cover the entire problem.
- Encompass all the constraints.
- Be simple and inclusive.

In its simplest from, optimization methods are concerned with finding a minimum or a maximum solution from a set of possible solutions. If the function $f(x) : A \rightarrow \mathrm{R}$, where

$f(x)$ is the objective function, and

A is a set of real numbers, or the search space.

The minimization problem is concerned with finding an element (x_0) in A where

$f(x_0) \leq f(x) \text{ for all } x \in A$ (This statement is a constraint)

The maximization problem is described as finding an element (x_0) in A where

$f(x_0) \geq f(x) \text{ for all } x \in A$ (This statement is a constraint)

Optimization problems can be classified according to different characteristics [46]. Some of the most significant classifications are

- Number of variables: single or univariate and multivariate problems.
- Type of variables: continuous-values and integer or discrete-valued variables.
- Linearity of the objective function: generally linear and non-linear.
- Constraints: constrained and unconstrained or boundary constraint.
- Optima: one-solution problems are called unimodal. Multi-solution problems are multimodal. Problems with false solutions are called deceptive problems.
- The number of objective solutions: single or multi-objective functions. Multi-objective functions have more than one criterion to optimize simultaneously.

Local optima are an area or a subset of the candidate solutions that will meet the constraint, but are all in the same area. A better solution (global optima) may exist outside of this area but still within the search space.

Figure 3.1 explains the idea of local and global optima. Assuming the objective function is to search for the minimum. The entire search space is A. B is a subset of A. The minima found in B are local optima. The global optimum is found outside of B but inside of A. Reference [46] also classifies the local optima into two categories, strong and weak optima. A strong minimum in this example would be the lowest of all local minima in B. Other minima in B that are not necessarily the lowest are weak minima.

One of the most common problems with the different kinds of optimization methods is how to be able to exit local optima. In this case, a “global” search method is more superior.

The fault location optimization problem, as applied to a real large-size power system needs a global search method. The fault location problem is a real problem with noise, multiple objective functions, and multiple possible solutions that are needed in the case of incorrect first candidate identified. The selection of the optimization method takes into account all the above considerations.

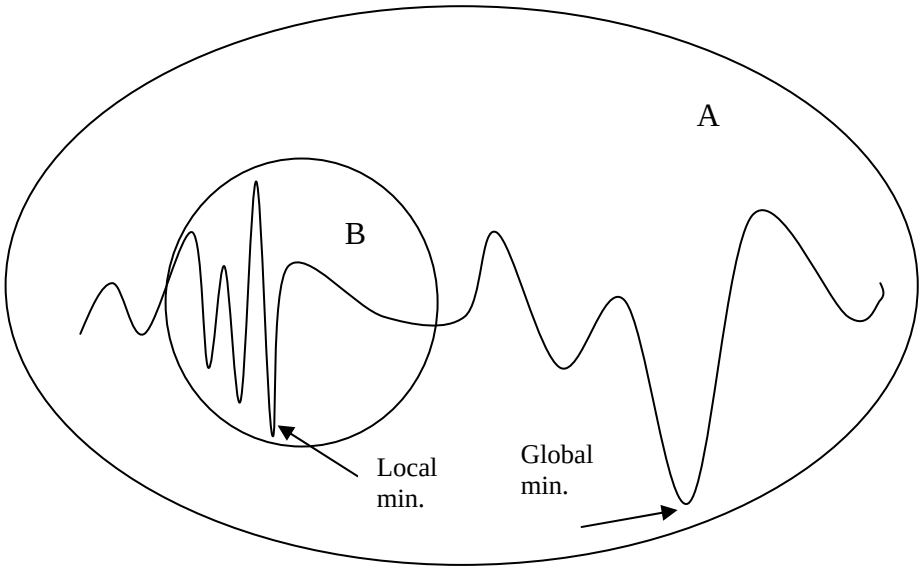

Figure 3.1 Global versus local optima

Optimization problems are subject to constraints. Constraints can be equality or inequality conditions. This has the effect of eliminating solutions that could have been otherwise considered global optima. For example, if we add a constraint to the problem in figure 3.1, as shown in figure 3.2, then the best solution becomes an extremum. Constraints can be equality (equal to a constant) or inequality (less than or equal to or greater than or equal to) constraints. The example, the constraint shown in figure 3.2 is an inequality constraint. It divides the search space into two spaces, a feasible space (greater than) and an infeasible space (less than or equal to). The global minimum found in figure 3.1 is no longer a valid solution as it lies in the infeasible space. The intersection of the objective function with the feasible search space as the objective function departs the infeasible space is now the new optimum solution. It is still a better optimum solution than the local minimum found previously.

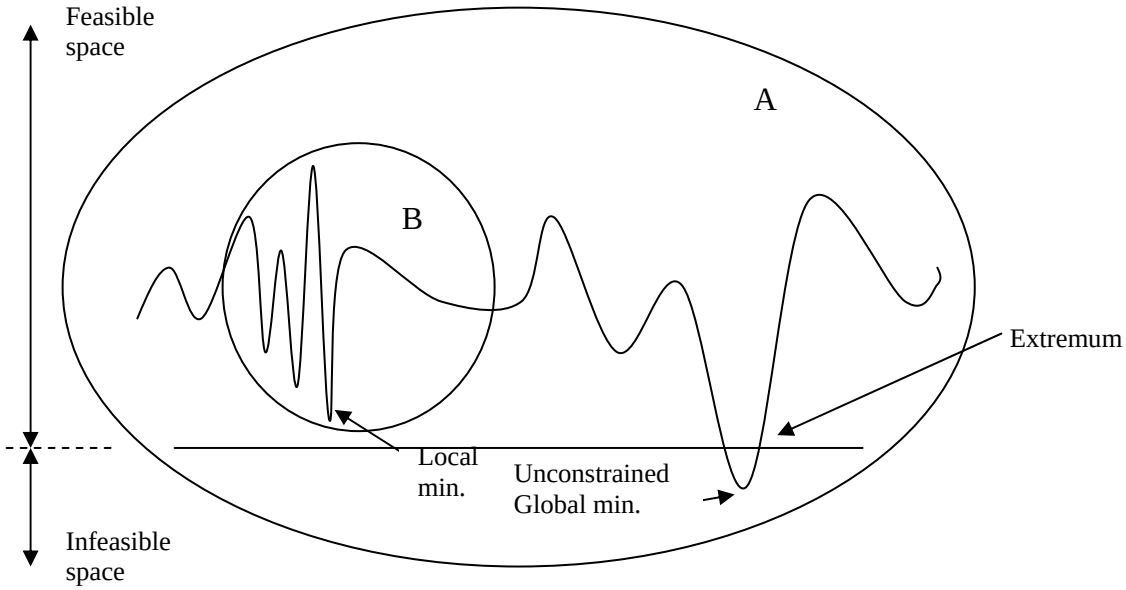

Figure 3.2 Global versus local optima (with constraint)

3.2 Review of Particle Swarm Optimization

Particle Swarm Optimization (PSO) is a computational intelligence-based optimization method that utilizes group behavior. Group behavior has been studied by researchers and simulations were attempted to simulate crowd behaviors such as flocks of birds, fish schools, ant colonies and other groups of animals that have complicated and complex collective behaviors. Studying this type of optimization method involves social science (psychology) and computer science [19]. It is an evolutionary technique that was developed around 1995 by Eberhart and Kennedy [20, 21].

A swarm of particles is basically a number or a group of individuals or particles (a population), each with a certain velocity, all roaming a particular search space. However, certain principles govern the swarm intelligence [22]. These principles are the proximity (ability to perform simple space and time computations), quality, diversity (in response), stability, and adaptability (when it is worth the computational effort).

Researchers have developed many different PSO algorithms. These algorithms are developed to solve different types of problems. This includes single-solution or multiple-solution algorithms, constrained-optimization problem algorithms, multi-objective problem algorithms, dynamic problem algorithms, and discrete PSO algorithms. The different PSO algorithms improve upon the basic PSO algorithm by enhancing convergence or diversity of the swarm.

Particle Swarm intelligence has been applied to several power system problems. This includes a variety of power system planning problems, such as power system security and contingency analysis [23, 24], state estimation [25], voltage and reactive power control [26-30], economic dispatch [31], power system expansion planning [32, 33], optimal power flow [34], and system protection [35]. In this research effort, another application is added. PSO algorithm is used in conjunction with synchrophasor quantities to locate transmission line faults.

The movement of a certain particle in a swarm is a function of its speed, the best position it ever attained, and the best position ever attained by any other particle in its swarm.

As stated earlier, PSO is a stochastic population intelligent algorithm that has been successfully adopted for solving large-scale nonlinear optimization problems in many areas of power system analyses [19]. Since PSO features a global searching ability and memory property, it can efficiently provide the best result as well as determine other possible candidate results. This property is very useful in real applications, where measured data could be biased for various reasons. In the fault location problem, other candidate results can reflect the actual fault location. Additionally, PSO algorithm is simple to implement and has very few parameters to adjust. These characteristics make PSO an intuitive choice to solve fault location problem in a real large-size power system.

The following section is an introduction to the basic PSO.

3.3 Basic PSO principles

As stated earlier there are many PSO algorithms that have been developed since its inception in 1995. The improved PSO algorithms deal with convergence and diversity of a swarm. The PSO algorithm is based on the swarm concept. Each particle of PSO represents a

candidate solution and has two properties: position (k_i) and velocity (v_i). The velocity of a particle directs the flight of the particle.

A population of particles, called a swarm, keeps flying around the search space until the stop criteria is satisfied. Initially, each particle in the swarm is randomly chosen in the searching space. Then, at each step, each particle is updated according to equations below. Notice that the standard PSO algorithm is modified into an integer-PSO for the purpose of fault location application.

$$v_i^{j+1} = wv_i^j + c_1 ran_1 (p_{best_i}^j - k_i^j) + c_2 ran_2 (g_{best}^j - k_i^j) \tag{3.1}$$

$$k_i^{j+1} = round(k_i^j + v_i^{j+1}) \tag{3.2}$$

$$k_i^0 \in U(k_{\min}, k_{\max})$$

$$w = w_{\max} - (w_{\max} - w_{\min})(\frac{j}{j_{\max}}) \tag{3.3}$$

Where,

j is the iteration index, it can also be regarded as the discrete time step.

w is the inertia weight,

k_i^j is the fault location vector of i^{th} particle at j^{th} iteration (or at time j),

U is the search space

v_i^j is the velocity vector of i^{th} particle at j^{th} iteration.

c_1 and c_2 are two positive constants,

ran_1 and ran_2 are two random numbers in range [0, 1],

$p_{best_i}^j$ is the best position of i^{th} particle after j iterations,

g_{best}^j is the best position of the whole swarm after the j^{th} iteration, and

$round$ rounds elements to the nearest integer.

In the above equations, it is clear that the next position of a particle is a function of its current location and velocity. Referring back to the previous velocity three-term equation, we note that velocity is updated every iteration (time interval). Velocity is a function of three components:

- First term: inertia or momentum. It is the tendency to remain in the same direction. This is basically related to the existing velocity.
- Second term: linear movement towards the best position ever found by a particular particle. Also called memory or self knowledge. Some researchers referred to this term as "nostalgia" of the particle [36].
- Third term: linear movement towards the best position found by any particle in the neighborhood, or the swarm if the neighborhood consists of the entire swarm. Also known as cooperation or group knowledge. This is the social component of the swarm intelligence.

We also notice from the previous velocity equation that each one of the three terms is assigned a weight. The first term (inertia) is influenced by the inertia constant. This could be a fixed number or a dynamically changing number [37]. Dynamically changing the inertia constant is common. Reducing this constant (linearly or non-linearly) allows moving from an exploratory mode to an exploitative mode. However, this causes the algorithm a decreased ability to explore new areas [19]. Other methods may linearly or non-linearly increase this constant, randomly change it, or control it adaptively.

c_1 and c_2 constants, coupled with the ran_1 and ran_2 numbers, contribute to the second and third term respectively. Small values will cause small effect. Generally, a value of $c_1 + c_2 = 4$ has been suggested [38, 39]. Usually, most applications use $c_1 \approx c_2$. It is worthwhile to note that many PSO algorithms have maximum velocity limits.

To initialize the PSO algorithm, the initial positions of the particles have to be provided. Additionally, acceleration constants (as discussed previously), initial velocities, and personal

best positions have to be provided. Initial velocities can be assumed zero (do not have to have a random value). The particle's best position is initialized at the particle's position at time zero (before iterating starts).

Diversity of the initial locations of the particles in the search space will ensure better convergence in less iteration. It also helps escape local optima. It is suggested that particles will uniformly cover the search space. This improves efficiency and helps avoid having to provide enough inertia to be able to move particles in order to find a solution in an uncovered region.

During iteration, an objective function is evaluated, and a fitness value is calculated. The function is evaluated for each particle and therefore, the global best position is found. The global best position is then used in finding the next velocity of each particle and determining its new location in the swarm.

Stopping the PSO algorithm can be accomplished in many different ways. These usually include:

- After a maximum number of iterations. This method is simple. Experience using it in the fault location problem showed good results as the number of iterations needed for fault location has been relatively low. However, generally a small number of iterations may stop the algorithm before acceptable results are reached. Too many iterations increase the computational burden.
- An acceptable solution is found. This usually means that the error in the objective function is less than a pre-specified value. This is hard to implement in a real-world application where error is built into the signal being measured. In the fault location problem, the synchrophasor measurement error is unknown, and can assume different values within or outside the total vector error (TVE) as specified in standard IEEE C37.118.

- If the particles stop changing position by more than a pre-specified value (particle speeds are approaching zero). In fault location method, this is not necessarily where the fault location might be.
- When the particles are too close to each other (also know as swarm radius method or the clustering approach). This is not necessarily the case in fault location as experience showed that the candidate solutions can be far from each other. It is also possible to terminate too early in this case.
- When the rate of change of the objective function approaches zero. This method may get the algorithm stuck in a local optimum.

For g_{best}^{j}, the neighborhood is the entire swarm. The social network for the swarm is a fully connected mesh topology. Fully connected mesh topology network for a five particle swarm is shown in figure 3.3. In this topology, each individual, or particle, is connected to all other individuals. Because each particle knows the best position of all other particles, this structure tends to converge quickly, but is susceptible to being trapped in local optima.

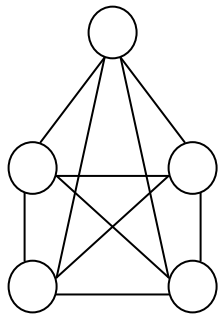

Figure 3.3 Fully connected mesh network topology

It shall be noticed that many network topology structures maybe utilized for global best position. A ring topology network will yield a neighborhood that is not the entire swarm. The swarm is divided into multiple neighborhoods that overlap. This intersection helps share information among neighborhoods. This is referred to as local best l_{best}^{j}. Figure 3.4 shows a

ring topology network. Many other social structures have been used by the researchers in the basic PSO algorithm. These structures include simple and complex structures.

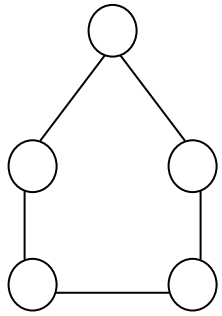

Figure 3.4 Ring network topology

In summary, the PSO algorithm uses the following general process in reaching a solution. First, the user defines multiple parameters, such as the swarm and neighborhood population, the number of iterations (if constant), and the acceleration constants. Then, the algorithm is initialized using random or uniformly distributed positions of the particles in the swarm. Following this, the objective function is evaluated for every particle. The best position for each particle is found. The best position of all particles in the swarm is also found. Next, the velocity and position of each particle is updated using equations (3.1) and (3.2). Each particle assumes a new position. This is repeated every iteration, until a particular stop criteria is reached.

PSO explores multiple solutions in parallel and utilizes a cooperative manner. Additionally, the PSO algorithm does not require an accurate initial guess. In the fault location problem, this means that there is no need to identify the faulted line. PSO has the ability to escape from local optima, which make it suitable for fault-location.

CHAPTER 4

THE PROPOSED FAULT LOCATION METHOD

4.1 Introduction

In this chapter, a new proposed method for fault location is presented. The proposed method consists of three steps. Step one identifies the impacted area of a large power system based on synchronized phase angle measurements. This is referred to as disturbance-area identification. Using conclusions on the affected parts of the system, step two reduces the system to a small number of buses, and calculates the bus admittance matrix and bus impedance matrix of the reduced system. This is referred to as dynamic power system reduction. Step three applies a positive sequence voltage method and particle swarm optimization to identify the candidate fault locations. In the next sections, each step is explained in detail.

4.2 Disturbance-Area Identification

Voltage phase angle measurements taken from different parts of the system reflect the state of rotor angle swings in these areas following a system disturbance. With faults closer to generator terminals, swing acceleration is higher [6]. This is reflected on phase angle measurements taken at transmission buses. If the system is divided into areas that are connected through tie lines, each PMU area is thought of as a sub-network that consists of multiple machines that swing together and have small voltage angle differences. To simplify the analysis, we assume uniform damping [6]. All generators in area A are described in the following swing equation,

$$M_A \ddot{\delta}_A + D_A \dot{\delta}_A + \sum_{i \in I_A} P_{Gi} = \sum_{i \in I_A} P_{Mi}^0 \tag{4.1}$$

Where,

$M_A = \sum_{i \in I_A} M_i$,

$M_i = H_i / \pi f_0$, H_i is the inertia constant of generator i ,

δ_A is the center of angles for area A ,

$D_A = \sum_{i \in I_A} D_i$,

D_i is the damping constant of generator i ,

P_{Gi} is the instantaneous power of generator i , and

P_{Mi}^0 is the mechanical power supplied by turbine of Generator i .

δ_A is unknown, but we assume it is equal to the voltage phase angle of area A PMU. We assume that $\delta_A = \delta_{A0}$ prior to the disturbance. During the fault, the above energy balanced is disturbed, P_{Gi} decreases suddenly, while P_{Mi}^0 cannot change instantly. This causes δ_A to accelerate. After circuit breakers trip to remove the faulted line, δ_A starts to decelerate (P_{Gi} is greater than P_{Mi}^0) until the kinetic energy gained during acceleration is expended at $\delta_{A\,swing}$, then δ_A starts to decrease. If the system is transiently stable, this swing behavior converges to a new steady state. We define angle swing for area A as:

$$\Delta\delta_A = \left| \delta_{A\,swing} - \delta_{A0} \right| \tag{4.2}$$

This concept is used to perform initial screening of the PMU measurements to identify the impacted areas of the system. If we ignore the differences in inertia and damping across the different PMU measurement areas, the areas with the greatest angle swing are identified as impacted areas, and are examined closely for the fault location. Areas with negligible swing

angle are replaced with an equivalent. Most transient faults do not affect a large area of the power system.

4.3 Dynamic Power System Reduction

After the impacted areas of the system are identified, the system can be reduced to maintain all or parts of the impacted areas. The choice of which buses to keep in the reduced model can be automated by assuming a multiple layer system, where layer 0 includes the PMU measurement bus, or by creating bus subsystems for each PMU area that will be maintained in the reduced model. Node reduction of the admittance matrix of the system using Gaussian Elimination is the basis for this method.

The large system is reduced to a manageable number of buses. Often, detailed models include several buses at one electrical node. Combining all the buses from each group of buses at the coherent area and same voltage level will greatly reduce the equivalent system model. Assuming an n bus system is to be reduced to an $n-l$ bus system, then the admittance matrix is rearranged to locate the buses to be retained at the bottom of the matrix as follows

$$\begin{bmatrix} Y_{11} & \cdots & Y_{1l} & \cdots & Y_{1n} \\ \cdots & \cdots & \cdots & \cdots & \cdots \\ Y_{l1} & \cdots & Y_{ll} & \cdots & Y_{ln} \\ \cdots & \cdots & \cdots & \cdots & \cdots \\ Y_{n1} & \cdots & Y_{nl} & \cdots & Y_{nn} \end{bmatrix} \begin{bmatrix} V_1 \\ \cdots \\ V_l \\ \cdots \\ V_n \end{bmatrix} = \begin{bmatrix} I_1 \\ \cdots \\ I_l \\ \cdots \\ I_n \end{bmatrix} \tag{4.3}$$

Node 1 can be combined using the following equations,

$$Y_{i,j}^{new} = Y_{i,j}^{old} - \frac{Y_{i,1}^{old} Y_{1,j}^{old}}{Y_{11}^{old}} \quad where\, i, j = 2,...,l \tag{4.4}$$

$$I_i^{new} = I_i^{old} - \frac{Y_{i,1}^{old}}{Y_{11}^{old}} \quad where\, i = 2,...,l \tag{4.5}$$

The two equations above are repeated until the (n,n) admittance matrix is reduced to an $(n-l,n-l)$ admittance matrix. The voltages are the same at the retained buses as they were before the reduction operation, however, the currents are "redistributed" during this process.

4.4 Fault Location Method

Several algorithms have been developed for fault location. Most algorithms utilize single or dual-ended voltage and current quantities to locate faults. In Chapter 2, several fault location methods were discussed. For quick review, a quick summary is provided. References [12] and [41] provide accurate methods for dual-ended fault locating using currents and voltages. Such a method does not require knowledge of the system outside of the faulted line, and usually include no simplifying assumptions. However, typical challenges to this type of method are communication to both ends of the line, and minimizing or eliminating effects of some factors such as fault resistance, current distribution factors and load. A negative sequence fault location method has been developed in [43]. This method claims to be immune to load, zero-sequence mutual coupling, current infeeds, and fault resistance, but would require measurements at each end of the faulted line. Single-ended algorithms have been widely examined as in [9, 10] and [42]. These are simple methods. Typical challenges are fault resistance, load and other simplification assumptions. If source impedance is used, then it is subject to change due to the power system changes. Other fault location methods include short circuit data matching to the short circuit model and traveling wave methods.

In the recent years, utilities have started installing PMU measurements across their systems. However, many utilities still have very few synchrophasor points installed, which limits the application development to take advantage of these installations. Different utilities are recording different quantities and at different sampling speeds. Most utilities record voltages but may not record currents. They may record only positive sequence quantities.

Recently, voltage-only methods have been suggested in [4, 5]. These methods assume the availability of the impedance matrix of the system Z_{bus}. Practically, this matrix is not usually calculated. Extraction of certain rows and columns is possible, but still requires large matrix manipulations. With the use of the reduction methods discussed in sections 4.2 and 4.3 of this Chapter, the use of Z_{bus} is possible. In this case, a simple optimization search can be done on the reduced system. The following discussion describes the basis for the new synchrophasor voltage-only fault location method.

During pre-fault conditions on the system

$$\left[V^0\right] = \left[Z_{bus}\right]\left[I^0\right] \tag{4.6}$$

During fault conditions, the current changes by ΔI and the above equation becomes

$$\left[V\right] = \left[Z_{bus}\right]\left[I^0 + \Delta I\right]$$

$$\left[V\right] = \left[V^0\right] + \left[Z_{bus}\right]\left[\Delta I\right]$$

$$\left[V\right] - \left[V^0\right] = \left[\Delta V\right] = \left[Z_{bus}\right]\left[\Delta I\right] \tag{4.7}$$

We assume the fault current to be injected into the system at fictitious bus k as shown in figure 4.1. The faulted line connects buses m and n. The fault location method assumes the availability of at least two PMU measurements in the impacted areas. We assume PMU points installed at buses r and s. The per unit distance of the fault from bus m is d.

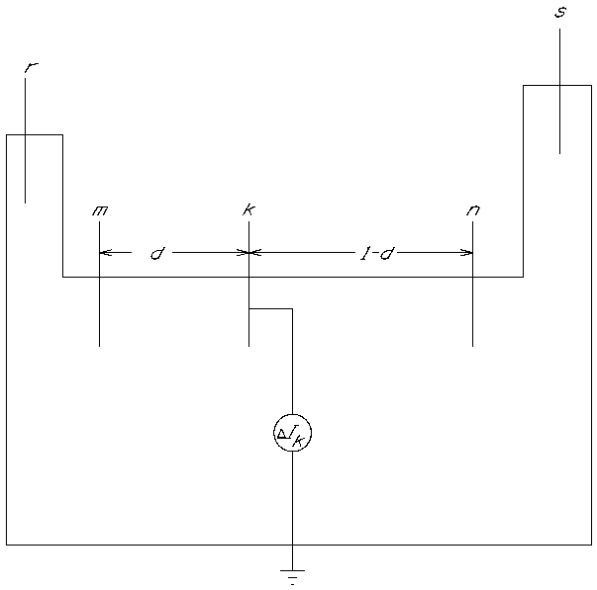

Figure 4.1 Positive sequence one-line diagram of faulted line (m-n) with fictitious fault bus k and PMU buses r and s

Applying equation (4.7) to a large system with the buses shown in figure 4.1 results in the following voltage changes

$$\begin{bmatrix} \Delta V_1 \\ \Delta V_2 \\ \cdots \\ \Delta V_r \\ \cdots \\ \Delta V_m \\ \cdots \\ \Delta V_n \\ \cdots \\ \Delta V_s \\ \cdots \\ \Delta V_k \end{bmatrix} = \left[Z_{bus\,\mathrm{mod}} \right] \begin{bmatrix} 0 \\ 0 \\ \cdots \\ 0 \\ \cdots \\ 0 \\ \cdots \\ 0 \\ \cdots \\ 0 \\ \cdots \\ \Delta I_k \end{bmatrix} \tag{4.8}$$

Where $Z_{bus\,\mathrm{mod}}$ is a modified Z_{bus} with added fault bus k.

The modified bus impedance matrix can be obtained by directly modifying the existing bus impedance matrix using Z_{bus} modification procedures or by modifying the bus admittance matrix and inversing it to get the modified bus impedance matrix. Procedure to perform this are discussed in many textbooks including [7]. The method chosen here is to modify the admittance matrix to add the new fault bus. This is because the matrix inversion is not computationally expensive for such a small system. After obtaining a Y_{bus} for the selected reduced system, it is only necessary to modify a limited number of elements to obtain $Y_{bus\,\mathrm{mod}}$. If the new fault bus is k, we assume the fault bus is located at distance d from bus m and distance $1-d$ from bus n as shown in figure 4.1. Only very few elements of Y_{bus} are modified to form $Y_{bus}^{'}$. The following relationships can be obtained:

$$Y_{mk} = -\frac{y_{mn}}{d}$$

$$Y_{nk} = -\frac{y_{mn}}{1-d}$$

$$Y_{mm}^{'} = Y_{mm} - y_{mn} + \frac{y_{mn}}{d} = Y_{mm} - (1-\frac{1}{d})y_{mn}$$

$$Y_{nn}^{'} = Y_{nn} - y_{mn} + \frac{y_{mn}}{1-d} = Y_{nn} - (1-\frac{1}{1-d})y_{mn}$$

$$Y_{mn}^{'} = 0$$

$$Y_{nm}^{'} = 0$$

Where

$Y_{mn} = Y_{nm} = -y_{mn}$ and,

$Y_{km} = Y_{mk}$

Additionally, a new row and a column are added to Y'_{bus} to create $Y_{bus\,\mathrm{mod}}$. The new row is

$$\begin{bmatrix} 0 & \cdots & Y_{mk} & \cdots & Y_{nk} & \cdots & Y_{k-1\,k} \end{bmatrix}$$

Where all row elements are zeros except those shown. The new column is

$$\begin{bmatrix} 0 \\ \cdots \\ Y_{mk} \\ \cdots \\ Y_{nk} \\ \cdots \\ Y_{k-1\,k} \end{bmatrix}$$

Then, we can find $Y_{bus\,\mathrm{mod}}$

$$Y_{bus\,\mathrm{mod}} = \begin{bmatrix} Y'_{bus} & \text{new column} \\ \text{new row} & Y_{kk} \end{bmatrix} \tag{4.9}$$

Finally, $Z_{bus\,\mathrm{mod}}$ is the inverse of $Y_{bus\,\mathrm{mod}}$.

Applying equation (4.8) discussed earlier to buses r and s of Figure 4.1,

$$\Delta V_s = Z_{s,k} * \Delta I_k \tag{4.10}$$

$$\Delta V_r = Z_{r,k} * \Delta I_k \tag{4.11}$$

$$f(k)_{r,s} = \frac{\Delta V_r}{\Delta V_s} = \frac{Z_{r,k}}{Z_{s,k}} \tag{4.12}$$

Where $f(k)_{r,s}$ is the fault location parameter for fault at bus k as calculated from PMU buses r and s.

4.5 Applying PSO to Fault Location

The particle swarm optimization algorithm (PSO) and its main concepts were discussed previously in Chapter 3. Ideally, the fault branch and distance can easily be estimated using fault location parameters discussed in the previous section. However, for an ordinary power system with many lines, this task is cumbersome. Recently, Particle Swarm Optimization (PSO), which is a stochastic population intelligent algorithm, has been successfully adopted solving large-scale nonlinear optimization problems in many areas of power system analyses [19]. Some of the benefits of applying the PSO algorithm to the fault location problem are

- Group knowledge allows for escaping local optima.
- No "good" initial guess is needed. This also means that there is no need to identify the faulted line.
- Very few parameters to adjust. Good typical values of these parameters is almost standard and they do not affect the results drastically
- Stop Criteria can be a minimum value of the object function or a maximum number of iterations. Utilizing real PMU data will produce a varying error. Therefore, a maximum number of iterations is suggested for this application.

PSO features a global searching ability and memory property. It can efficiently provide the best result as well as determine other possible candidate results. This method will produce and rank several candidates based on the objective function. Possibility of choosing a second best result is still available for large-scale systems. This property is very useful in real applications, where measured data could be biased for various reasons. Errors in the measured data can result in multiple solutions and results errors. Other candidate results can reflect the actual fault location.

The above characteristics make PSO an intuitive choice to solve fault location problem in this dissertation.

The objective function of the fault location problem can be formed as

$$L(k) = \sum_{n=1}^{M} \left\| \frac{\Delta V_r}{\Delta V_s} - \frac{Z_{r,k}}{Z_{s,k}} \right\| \tag{4.13}$$

Where,

$M = C_2^N$ are all the possible combinations of fault location parameters using N PMUs,

r and s are defined as buses in the reduced model with PMU installations, and

k is the fictitious bus inserted at the fault location.

The above objective function allows for using this method with any number of synchronized voltage measurements.

The above method can be used to locate faults on a transmission line with synchrophasor measurement points on both ends with or without the need for additional synchronized phasor measurement readings elsewhere on the system.

4.6 Flow Chart of Fault Location Method

The new fault location algorithm flows as follows:

1. Disturbance-Area Identification: voltage phase angle measurements taken from different parts of the system reflect the state of rotor angle swings in these areas following a system disturbance. With faults closer to generator terminals, swing acceleration is higher. This is reflected on phase angle measurements taken at transmission buses. Each PMU area is thought of as a sub-network that consists of multiple machines that swing together and have small voltage angle differences (assuming uniform damping).
2. The areas with the greatest angle swing are identified as impacted areas. Areas with minimal change in Angle Swing are “equivalenced” in the reduced model. Note that the equivalencing process allows for transfer impedances to account for the equivalenced parts of the system. The equivalencing is done using the Gaussian Reduction method explained in section 4.3.

3. Using the fault location parameters explained in section 4.4, and the PSO algorithm explained in Chapter 3, the objective function for the PSO optimization is formed as shown in 4.5. The algorithm shall provide a list of ranked candidate solutions with the fitness value (residue quantity).

The flow chart for the proposed algorithm is shown in Figure 4.2.

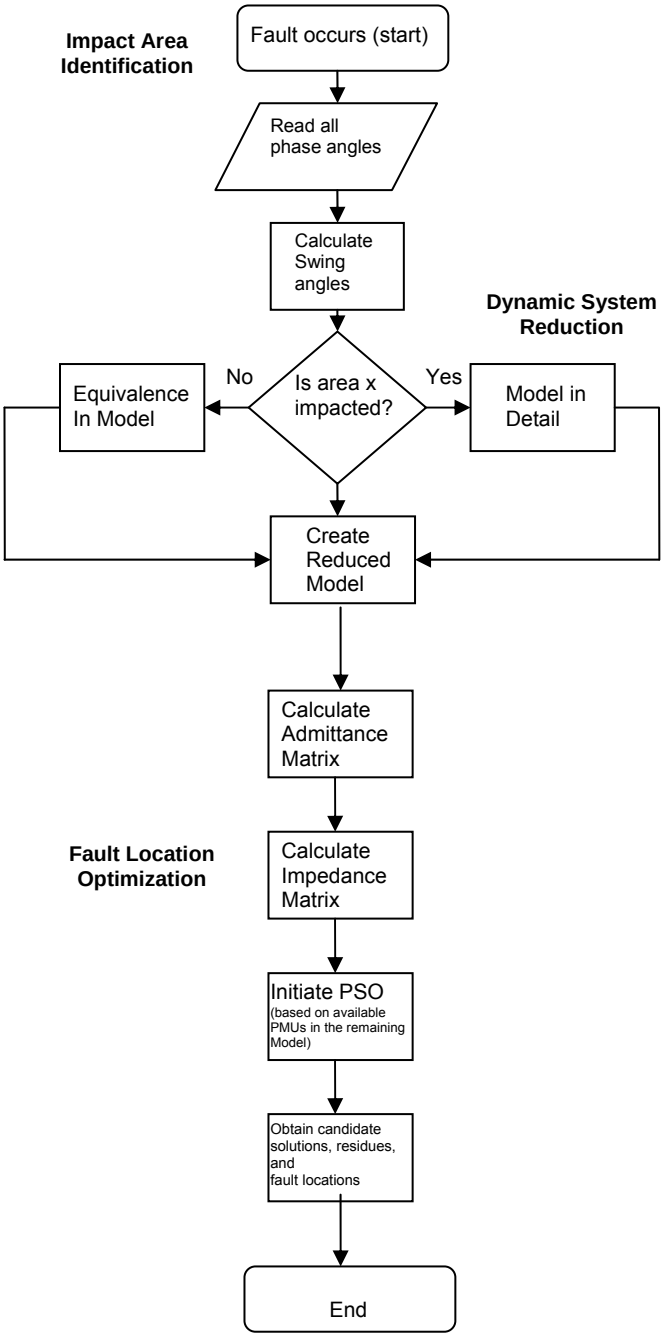

Figure 4.2 Flow chart of the proposed algorithm

4.7 Fault Location Method Summary

Researchers examined voltage-only methods using synchronized (or non-synchronized) quantities for many years. As the global positioning system (GPS) clock technology matured and became affordable, obtaining synchronized phasor measurements became feasible. Researchers also suggested the use of the bus impedance matrix for the fault location problem. The bus Impedance matrix is usually obtained by inversing the admittance matrix. Because of the size of such a matrix for a practical system (typically on the magnitude of thousand of rows and columns), the bus impedance matrix is not usually obtained as it will require inversing a large matrix. Textbooks suggest methods (i.e. triangular factorization) to extract certain rows and columns of a matrix. This is also not practical here because it still requires large size matrix operations as all or most or a large number of elements is needed.

In the new proposed fault location method, phasor measurement units are utilized to determine parts of the system to be included in a “reduced model”. The large size power system is divided into PMU areas or subsystems, and then the impact of a disturbance is determined by the change in the voltage phase-angle. Next, Gaussian Reduction is utilized to reduce the system to a manageable number of buses and particle swarm optimization Method is used to perform the search for the fault location candidates.

CHAPTER 5

APPLYING THE PROPOSED METHOD ON A LARGE POWER SYSTEM

5.1 Introduction

In this chapter, the new proposed method for fault location is applied to an actual power system in North and West Texas. PMU data is collected from different parts of the system and examined to explore the feasibility of the new method.

Figure 5.1 shows the map of North and West Texas with the locations of the different PMU installations across the system. The system is divided into 7 different areas with one or more measurements at each location. Multiple cases are discussed in the following subsections. Areas 1 and 2 of this system are of a very high wind generation intrusion and are parts of the Competitive Renewable Energy Zoning (CREZ).

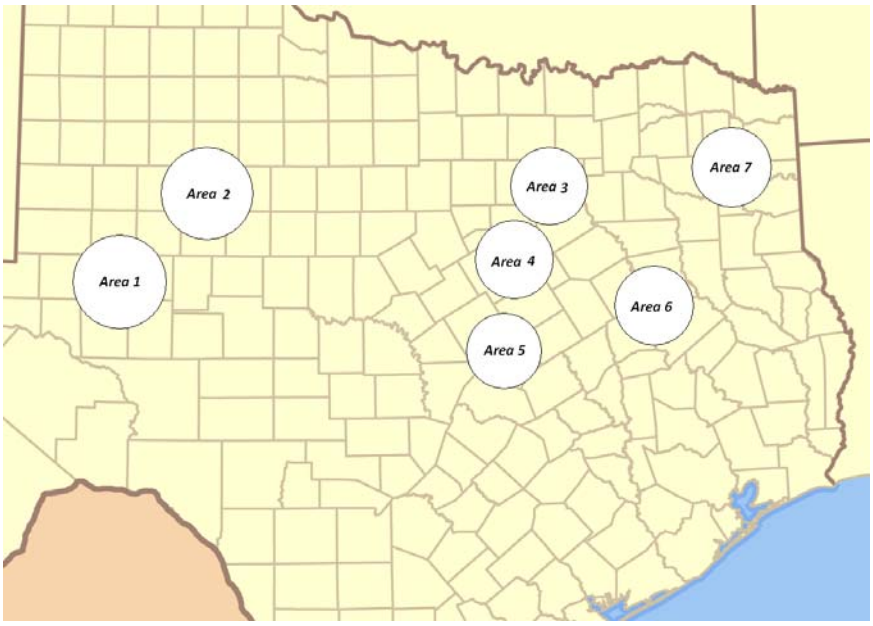

Figure 5.1 Divided Subsystem in North and West Texas

Table 5.1 shows the distribution of PMU devices that are connected to a centralized phasor data concentrator in this example system. It is noticed that areas 1 and 2 are

geographically close and have three measurements that are installed. Hence, the western part of the system is used to illustrate this method using test cases and real faults that occurred on this part of the system.

Table 5.1 PMU Installations per Area

Area	Number of installed PMUs
1	2
2	1
3	3
4	1
5	1
6	1
7	1

Figure 5.2 shows a sketch of the overall PMU system layout. The synchronized phasor measurements are taken at the station level using microprocessor based transmission line protective relays. This data is transmitted through Ethernet, radio, microwave, telephone modem, or a combination of these methods to a central phasor data concentrator. The data is then archived for off line analysis and used for visualization purposes as well.

In the next subsections, simulated faults and actual transmission line faults are provided. Results of the proposed fault location method are compared to two other methods and to the actual fault location (if known).

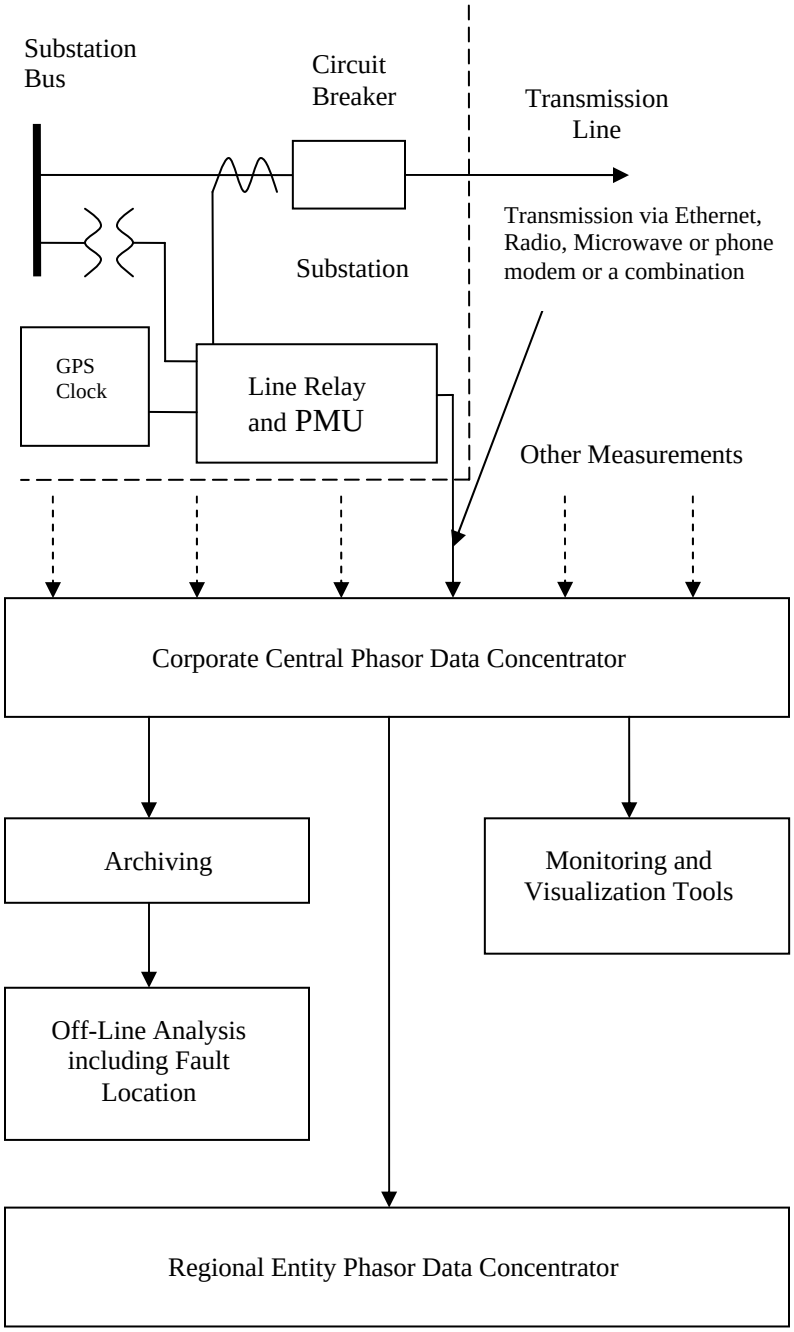

Figure 5.2 Sketch of the overall PMU network

5.2 Case Study 1

Some of the benefits of the proposed method are

- It uses positive sequence voltage. The positive sequence component is in all types of transmission line faults. Hence, this method can be used for any type of fault and no fault type identification is needed.
- This method uses ratios of the voltage, and therefore is current independent. This also means that the fault impedance should not cause significant error.

A reduced model is used for illustration purposes. This model includes parts of areas 1 and 2 in West Texas. Only the 345kV system is included in the reduced model. However, the reduced impedance matrix includes transfer impedances that account for the entire system. The reduced system is a 9-bus, 9-345KV line system as shown in Figure 5.3. These lines encompass a fairly large geographical area from east to west (about 130 miles).

In this case, the system introduced in Figure 5.3 is used to simulate some faults to test the performance of the new proposed method for different types of faults with difference fault impedances.

Table 5.2 shows the results of some simulations. It is noticed that the results are acceptable. The fault location error was high for unrealistically high fault impedance. In reality, high impedance faults are not very common on the transmission system. High resistance faults maybe more common on distribution voltages where there is more possibility of the conductor falling on the ground or a tree branch may cause the short circuit.

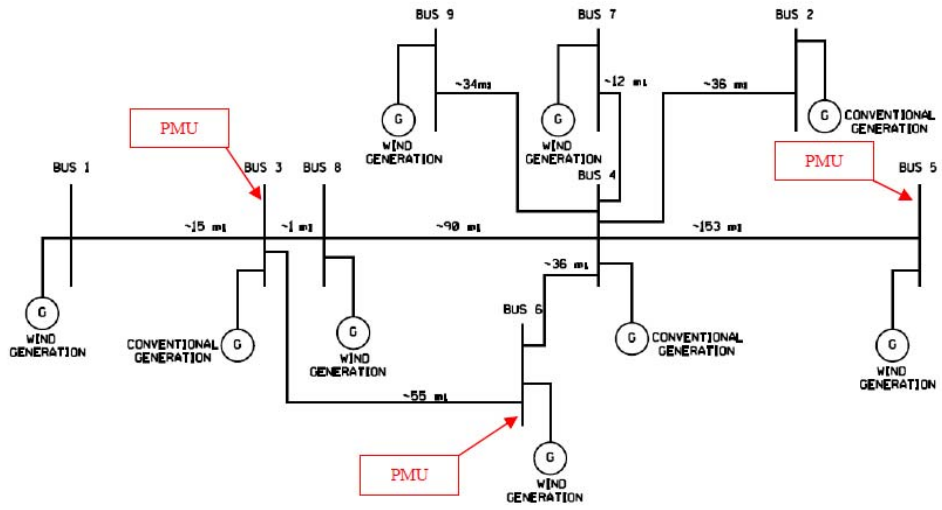

Figure 5.3 Single-line diagram of the reduced system in areas 1 and 2 in West Texas

5.3 Source Impedance Effect

We assume in this method that the algorithm has the correct bus impedance matrix it needs to perform the fault location search. This will be true if the algorithm is implemented in an environment where it has live updates to reconfigure the system bus impedance matrix. This makes an Energy Management System (EMS) the natural place to implement this algorithm. However, in this subsection, we would like to test the effect of source impedance changes on this algorithm, assuming it has been implemented in an isolated environment where it does not receive updates about the system configurations or operating conditions. If we repeat the first fault of the previous case (Table 5.2). The assumed fault is 0.15 per unit distance from bus 3 into the line 3-6. We will assume a 20% increase and decrease in the source impedance at bus 3 (closest to the fault) and bus 6 (second closest). It is noticed that a 20% change in source impedance at either end of the faulted line did not result in a significant error. Error was less than 1%. Table 5.3 summarizes the results.

Table 5.2 Case 1 Simulation Results

Fault on line from bus	To bus	Distance from the "From Bus" (%)	Fault Type	Fault Resistance (ohms)	Identified correct line	Identified Location (%)	Error (%)	Residue
3	6	15	A-G	0	Yes	15	0	0.00698629
3	6	30	A-G	50	Yes	31	1	0.046338
3	6	45	A-B-G	10	Yes	45	0	0.008913
3	6	60	A-B	2	Yes	60	0	0.011204
3	6	75	A-B-C-G	100	Yes	76	1	0.007856
1	3	50	A-G	0	Yes	47	3	0.00805
1	3	75	B-C-G	j100	Yes	71	4	0.003792
1	3	90	A-B-C-G	500	Yes, second candidate	98	8	0.061483
1	3	90	A-B-C-G	0	Yes	86	4	0.002737
At bus	8	0	A-G	0	Yes	1	1	0.009166
At bus	4	0	A-B-C-G	0	Yes	1	1	0.001371

Table 5.3 Source Impedance Effect

Bus	Source Impedance Change	Distance from the "From Bus" (%)	Fault Type	Identified correct line	Identified Location (%)	Error (%)	Residue
3	+20%	15	A-G	Yes	14	1	0.00744015
3	-20%	15	A-G	Yes	16	1	0.00703896
6	+20%	15	A-G	Yes	16	1	0.00703708
6	-20%	15	A-G	Yes	14	1	0.00702982

5.4 Case Study 2

In this case, actual synchrophasor data collected for a transmission line fault are used. This fault occurred on July 13th, 2011. Data from all PMUs described in Table 5.1 is provided. This data is then handled using Matlab to remove phase wrapping. The phase angle swing described in subsection 4.2 is applied to the obtained synchrophasor quantities. Table 5.4 summarizes the results. The fault is on the 345kV system. It is noticed that areas 1 and 2 are the only areas significantly impacted by this fault. Impact to area 1 is more than the impact to area 2. The voltage phase angle responses of areas 1 and 2 are shown in Figure 5.4. The voltage magnitude responses of areas 1 and 2 are shown in Figure 5.5. Sampling rate of the PMU measurements is 30 samples per second.

Table 5.4 Angle Swing for the Different PMU Locations

Area	PMU	$\Delta\delta$ (degrees)
1	1	0.4092
	2	0.4631
2	1	0.1325
3	1	0.0219
	2	0.0226
	3	0.0313
4	1	0.0519
5	1	0.0014
6	1	0.0073
7	1	0.0000

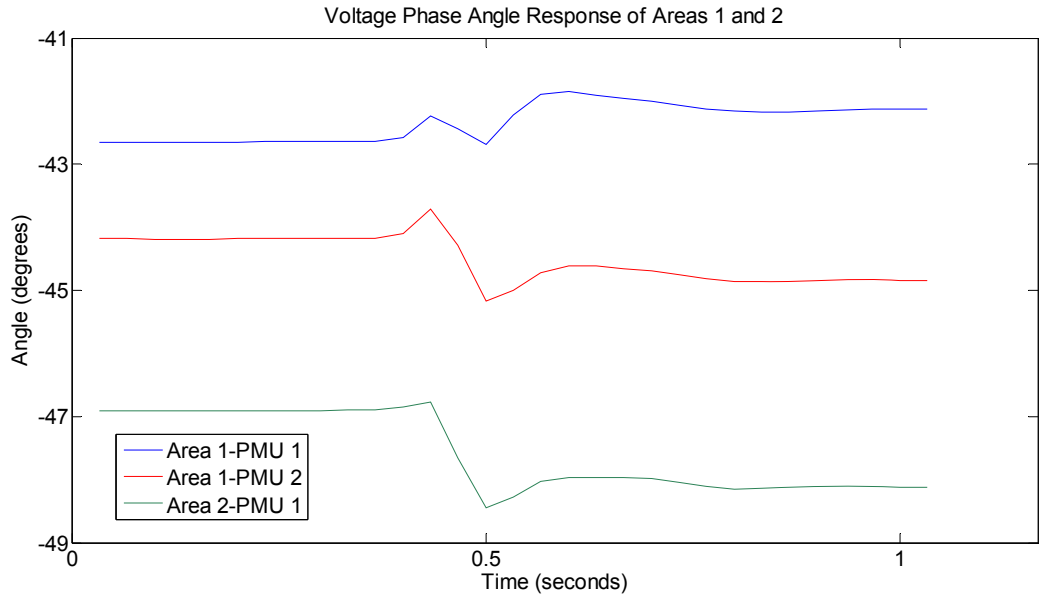

Figure 5.4 Voltage phase angle responses to the system fault

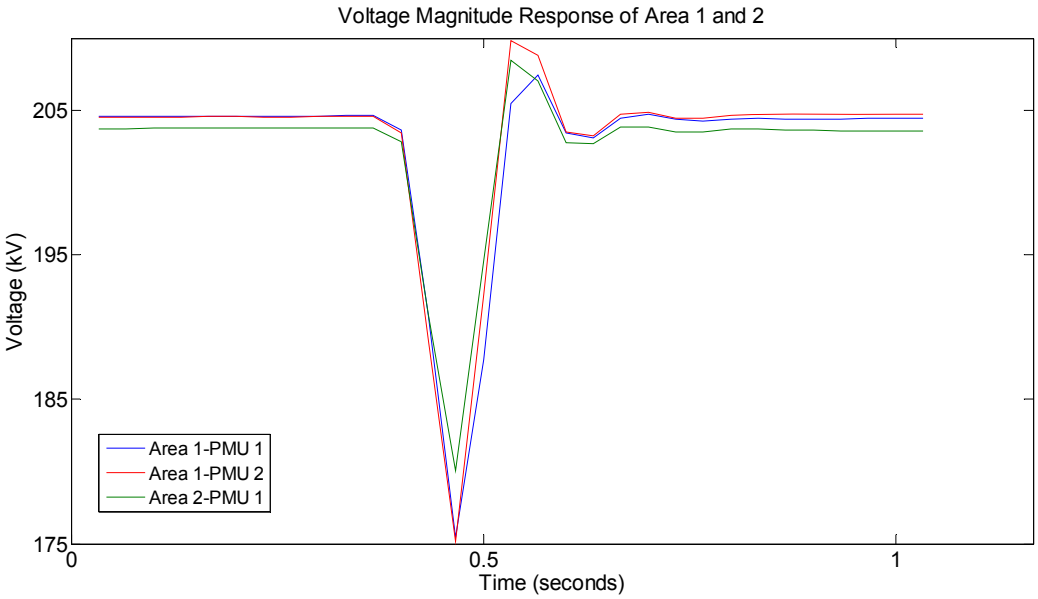

Figure 5.5 Voltage magnitude responses to the system fault

To be able to use more than two PMU quantities in the fault location algorithm, parts of area 2, especially those closest and tied to area 1 are modeled in detail in the reduced model. The reduced model is the same as that shown in Figure 5.3. The results of the PSO function

are shown in Table 5.5. The PSO algorithm optimizes the objective function as defined in subsection 4.5. The Residue is defined as

$$\text{Residue} = \left(\sum_{n=1}^{M} \left\| \frac{\Delta V_r}{\Delta V_s} - \frac{Z_{r,k}}{Z_{s,k}} \right\| \right) / \sum_{n=1}^{M} \left\| \frac{\Delta V_r}{\Delta V_s} \right\|$$

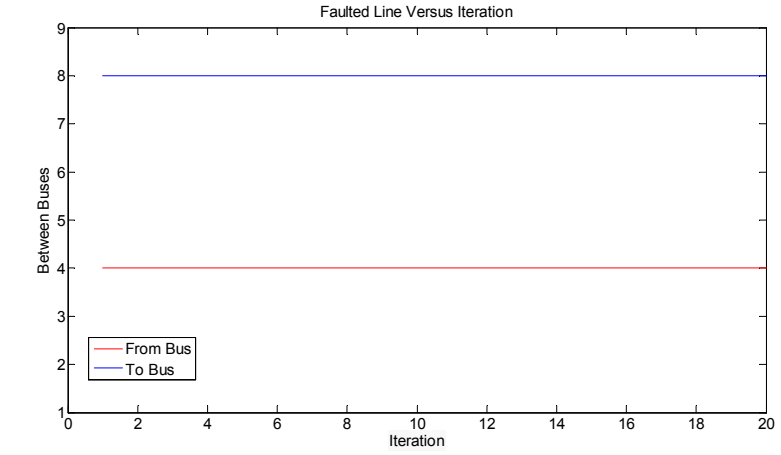

(a)

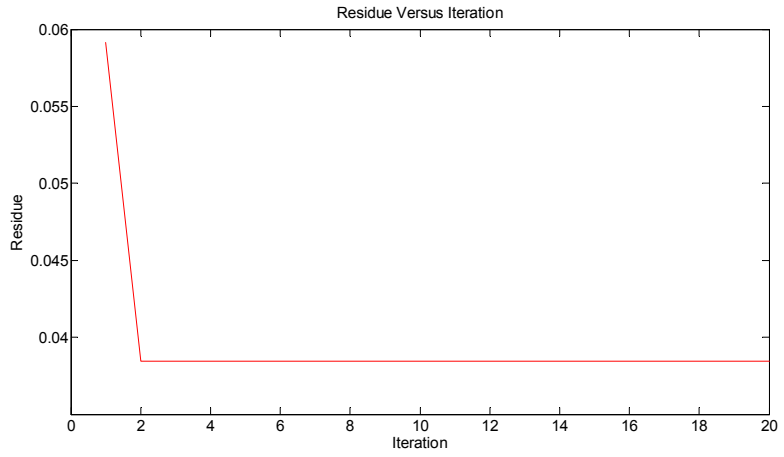

(b)

Figure 5.6 PSO iteration versus (a) identified faulted line (b) residue

Table 5.5 Particle Swarm Optimization Function Results

From bus	To bus	Location (%) from "From Bus"	Residue
4	8	30	0.038449
2	4	6	0.074412
4	6	9	0.416785
4	7	2	0.429881
4	9	1	0.431319
4	5	2	0.438905
5	9	93	0.629408
1	3	2	1.24159
3	6	36	1.25227

Figure 5.6(a) shows the iterations needed to identify the faulted line. Figure 5.6(b) shows the change in residue for each iteration step. It is noticed that the final solution is reached in as low as two iterations. The PSO algorithm located the fault between buses 4 and 8 at 0.30 per unit distance from bus 4. Only 0.01 per unit distance resolution is used in the algorithm. The faulted line decision is correct, as the fault happened on the identified line. Table 5.6 compares the results of this fault location method to two other methods and to the actual fault location. The First method is the single-ended fault location as calculated in the line terminal relays at bus 4. The second method is based on fault current matching using the short circuit model. PSO method produced adequate fault location for this fault. It is worthwhile to note that lines 3-6, 6-4, and 4-8 are mutually coupled for about 98% of the length of line 4-8. This fault was identified by the relay as an AC phase-to-phase fault. Following this fault, the line locked out of service. The fault was a result of heavy smoke during wild fires in West Texas.

Table 5.6 Comparison of PSO Method versus Other Methods

Method	Fault Location (per unit from Bus 6)	Error (%)
Single-Ended by relay at bus 4 (primary relay)	0.3060	0.44
Single-Ended by relay at bus 4 (backup relay)	0.3300	2.90
Short Circuit Model Match	Between 0.3400 and 0.3800	3.84
PSO	0.3000	0.16
Actual fault location	0.3016	

The normal fault clearing time is about 4 cycles. It is noticed that $\Delta\delta$ is reached in less than 6 cycles (3 samples). Table 5.7 compares the results for one sample, two samples (used to get values in Table 5.6), or three samples used. All results identify the faulted line successfully but with some difference in the location. This is because the PSO algorithm uses a ratio of voltages $\frac{\Delta V_r}{\Delta V_s}$. Most of the error created by sampling is removed in the division of the voltage changes if PMU locations are not very far from each other (the difference in angle acceleration is not great). However, the voltage error is a function of the PMU measurement device error and filtering algorithm. It is noticed that the minimum residue is obtained with 2 samples.

Table 5.7 Algorithm Performance for Different Time Intervals

Time (Samples)	From bus	To bus	Location from "From Bus"	Residue
1	4	8	0.27	0.048979
2	4	8	0.30	0.038449
3	4	8	0.36	0.044815

5.5 Case Study 3

This case is for another fault that happened on the 345kV system in West Texas. This fault happened on April 7th, 2011.

Table 5.8 includes results for the angle swing for different PMU areas for this fault. It is noticed that areas 1 and 2 are the only areas significantly impacted by this fault. The impact to area 1 is more than the impact to area 2. The sampling rate is 30 samples per second.

Table 5.8 Angle Swing for the Different PMU Locations

Area	PMU	$\Delta\delta$ (degrees)
1	1	0.8084
	2	0.9563
2	1	0.2907
3	1	0.0024
	2	0.0127
	3	0.0199
4	1	0.0446
5	1	0.0079
6	1	0.0334
7	1	0.0000

The voltage phase angle responses of areas 1 and 2 are shown in Figure 5.7. The voltage magnitude responses of areas 1 and 2 are shown in Figure 5.8.

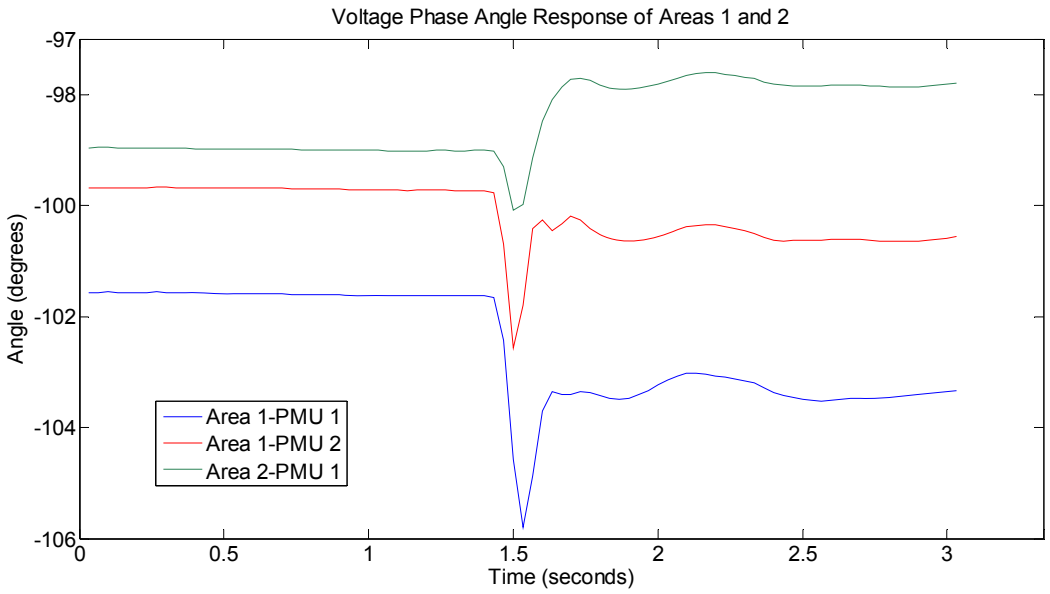

Figure 5.7 Voltage phase angle responses to the system fault

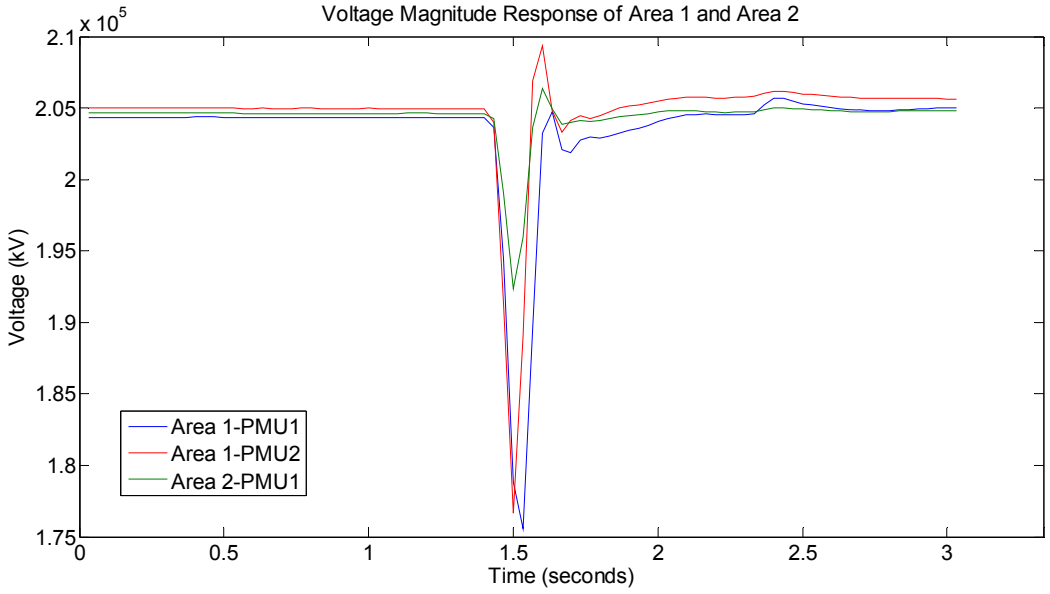

Figure 5.8 Voltage magnitude angle responses to the system fault

The same reduced system shown in Figure 5.3 is used for this case.

Table 5.9 Particle Swarm Optimization Function Results

From bus	To bus	Location (%) from "From Bus"	Residue
3	6	48	0.333918
4	8	58	0.357719
2	4	2	0.465263
4	6	55	0.468125
4	7	1	0.576995
4	9	2	0.579364
4	5	2	0.582328
1	3	2	0.587152
3	8	97	0.675449

Figure 5.9(a) shows the iterations needed to identify the faulted line. Figure 5.9(b) shows the change in residue for each iteration step. It is noticed that the final solution is reached in seven iterations. Table 5.9 shows the PSO algorithm results which located the fault between buses 3 and 6 at 0.48 per unit distance. Only 0.01 per unit distance resolution is used in the algorithm. The faulted line decision is correct, as the fault happened on the identified line.

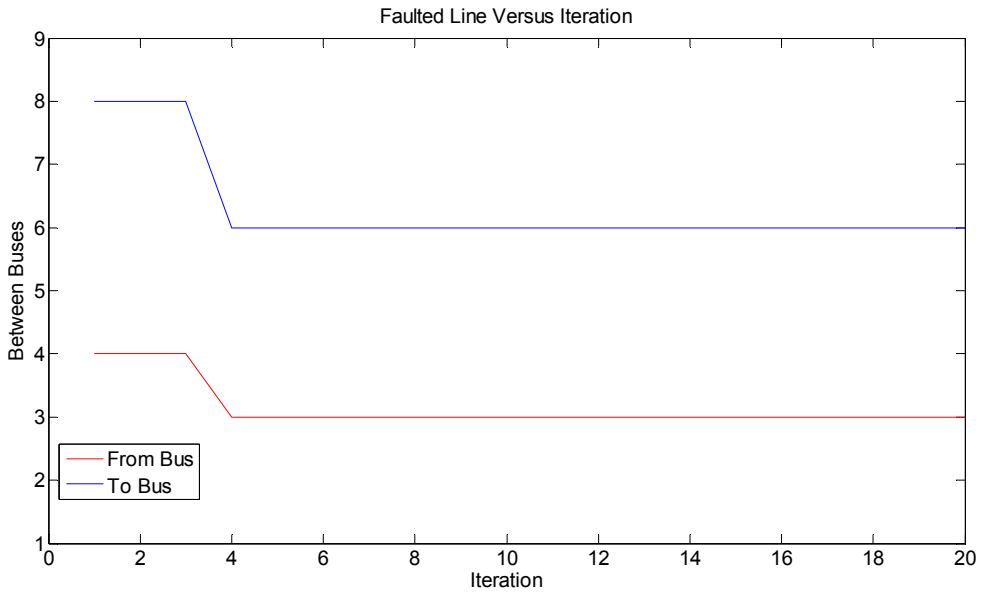

(a)

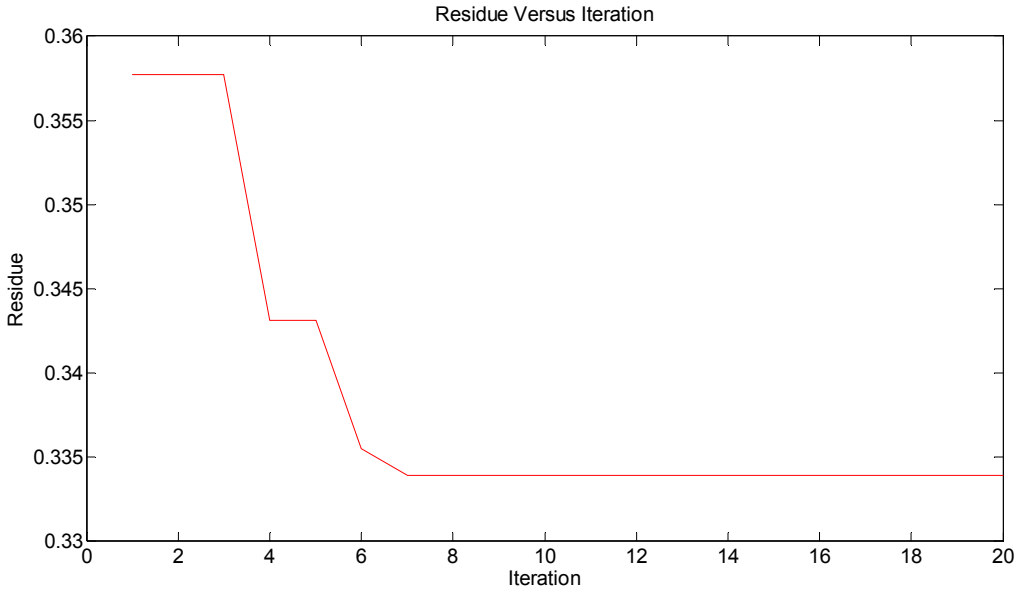

(b)

Figure 5.9 PSO iteration versus (a) identified faulted line (b) residue

Table 5.10 compares the results of this fault location method to two other methods. First method is the single-ended fault location as calculated in the line terminal relays at bus 3

and bus 6. The second method is based on fault current matching using the short circuit model. PSO method produced comparable fault location for this fault.

Table 5.10 Comparison of PSO Method versus Other Methods

Method	Fault Location (per unit from Bus 6)
Single-Ended by relay at bus 3 (primary relay)	0.49
Single-Ended by relay at bus 3 (backup relay)	0.51
Single-Ended by relay at bus 6 (primary relay)	0.43
Single-Ended by relay at bus 6 (backup relay)	0.44
Short Circuit Model Match	Between 0.44 and 0.45
PSO	0.48

5.6 Case Study 4

This case is for another fault that happened on the 345kV system in West Texas. This fault happened on October 22nd, 2010.

Table 5.11 includes results for the angle swing for different PMU areas for this fault. It is noticed that areas 1 and 2 are the only areas significantly impacted by this fault. The impact to area 1 is more than the impact to area 2. The sampling rate is 30 samples per second.

The same reduced system shown in Figure 5.3 is used for this case.

Table 5.11 Angle Swing for the Different PMU Locations

Area	PMU	$\Delta\delta$ (degrees)
1	1	0.8428
	2	1.0424
2	1	0.4243
3	1	0.0000
	2	0.0000
	3	0.0000
4	1	0.0308
5	1	0.0340
6	1	0.0000
7	1	0.0296

Table 5.12 Particle Swarm Optimization Function Results

From bus	To bus	Location (%) from "From Bus"	Residue
4	8	44	0.317052
2	4	1	0.40232
4	7	1	0.694475
4	9	1	0.695381
4	5	2	0.699242
4	6	2	0.702802
5	9	95	0.824339
1	3	11	1.14305
3	6	24	1.24385

Figure 5.10(a) shows the iterations needed to identify the faulted line. Figure 5.10(b) shows the change in residue for each iteration step. It is noticed that the final solution is reached in seven iterations. Table 5.12 shows the PSO algorithm results which located the fault between buses 4 and 8 at 0.44 per unit distance. Only 0.01 per unit distance resolution is used in the algorithm. The faulted line decision is correct, as the fault happened on the identified line.

Table 5.13 compares the results of this fault location method to two other methods. First method is the single-ended fault location as calculated in the line terminal relays at bus 3 and bus 6. The second method is based on fault current matching using the short circuit model. PSO method produced comparable fault location for this fault.

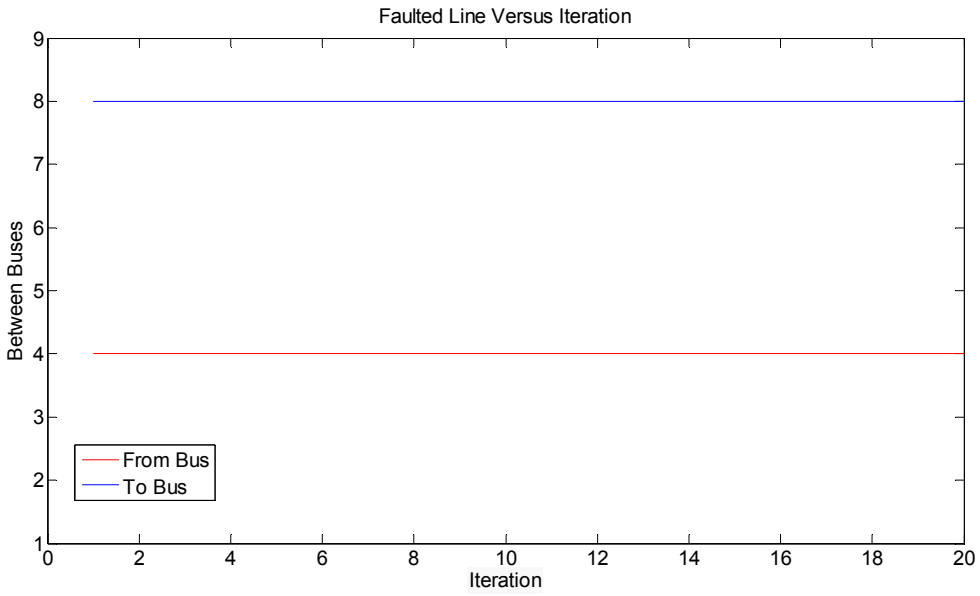

(a)

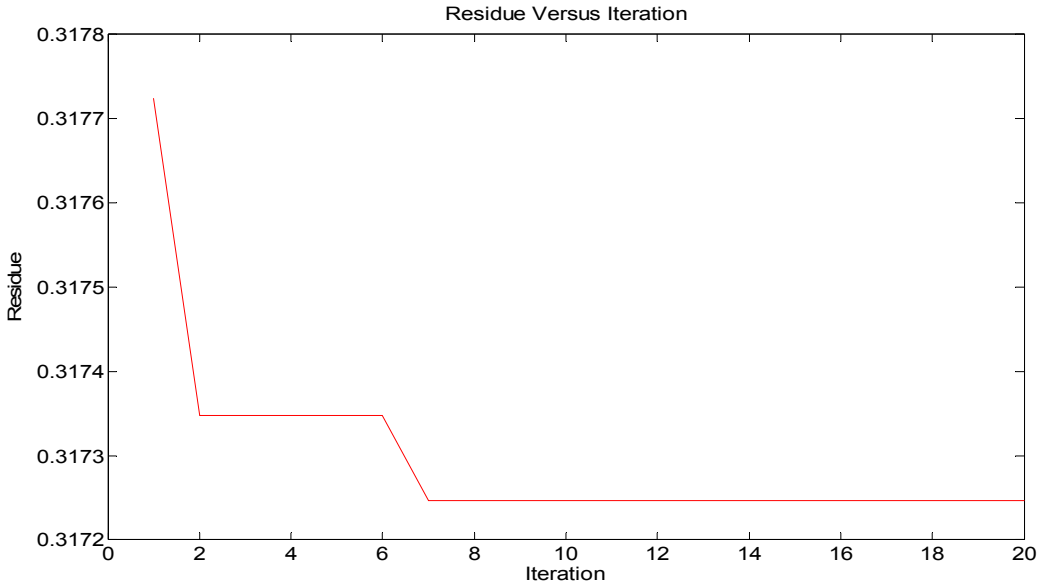

(b)

Figure 5.10 PSO iteration versus (a) identified faulted line (b) residue

Table 5.13 Comparison of PSO Method versus Other Methods

Method	Fault Location (per unit from Bus 6)
Single-Ended by relay at bus 8 (primary relay)	0.43
Single-Ended by relay at bus 8 (backup relay)	0.43
Short Circuit Model Match	Between 0.41 and 0.49
PSO	0.44

CHAPTER 6

CONCLUSIONS

6.1 Conclusion Remarks and Dissertation Contribution

In this dissertation, a new fault location method is proposed. This fault location method takes advantage of synchrophasor voltage quantities now available for use at some utility companies. It is understood that synchronized measurements are not available at every bus throughout a utility company. It is also understood that in many cases the utility company will choose not to record line current measurement because of the high number of branches and data logging, archiving, and handling concerns related to the large amounts of data. The proposed method utilizes voltage only synchrophasor measurement. It also does not require voltage synchrophasor quantities to be available at every bus.

The new method is based on an existing fault location parameters concept that has been proposed previously. In this dissertation, this concept is used in conjunction with the voltage angle swing concept to reduce the system used to search for a short circuit event. By reducing the system, calculating a reduced bus admittance matrix and a bus impedance matrix becomes feasible and practical. Next, particle swarm optimization method is used to efficiently search for the fault location. The search method is applied to this type of problem for the first time. This method is selected for various reasons, including a global searching ability and memory property (capability to escape local minima), the ability to efficiently provide the best result as well as determine other possible candidate results. This property is very useful in real applications, where measured data could be biased for various reasons.

The proposed algorithm is tested for actual transmission line faults in a large 345kV power system. Synchrophasor quantities from actual faults are used. The results are compared with other fault location results methods, including the short circuit database, and

distances of faults provided by the microprocessor relays available at the faulted line terminals. The results are promising.

6.2 Future Research

Several venues are possible for future research in this area to improve the accuracy of the proposed algorithm.

- Future verification and comparison of this method is needed as more faults (with a definite known location) occur on the system.
- The application of this method to zero sequence and negative sequence network and comparison of the results with the positive sequence for a variety of faults and network conditions.
- The application of this method to series compensated lines.
- The application of this method to locate faults on distribution system.
- The application of this method to a system with continuing updates from an energy management system, and integrating it with other synchrophasor display and analysis tools.

REFERENCES

[1] http://en.wikipedia.org/wiki/Phasor_measurement_unit

[2] K. E Martin, D. Hamai, M. G. Adamiak, S. Anderson, M. Begovic, G. Benmouyal, G. Brunello, J. Burger, Y. Song, C. Huntley, B. Kasztenny, and E. Price, “Exploring the IEEE Standard C37.118–2005 Synchrophasors for Power Systems,” IEEE Transactions on Power Delivery, Vol. 23, No. 4, October 2008.

[3] IEEE standard for synchrophasors for power systems, IEEE standard C37.118-2005, March 2006.

[4] Y. Liao, "Fault Location for Single-Circuit Line Based on Bus-Impedance Matrix Utilizing Voltage Measurements," IEEE Trans. Power Delivery, vol. 23, pp. 609-617, Apr. 2008.

[5] N. Kang and Y. Liao, "Fault Location Estimation for Transmission Lines Using Voltage Sag Data,” Power and Energy Society General Meeting 2010.

[6] A. Bergen, and V. Vittal, Power Systems Analysis (2nd ed.). New Jersey: 2000, p. 528-579.

[7] J. Grainger, and W. Stevenson, Power Systems Analysis, New Jersey, Tata McGraw-Hill: p. 238-328.

[8] C. Zimmerman, and D. Costello, “Impedance-based fault location experience,” 2005 58th Annual TAMU Conference for Protective Relay Engineers proceedings.

[9] T. Takagi, Y. Yamakoshi, M. Yamura, R. Kondow, and T. Matsushima, “Development of a new type of fault locator using one terminal voltage and current data,” IEEE Trans. Power Appar. Syst., Vol. PAS-101, No. 8 August 1982, pp. 2892-2898.

[10] L. Eriksson, M.M. Saha, and, G.D. Rockfeller, “An accurate fault locator with compensation for apparent reactance in the fault resistance resulting from remote end

infeed," IEEE Trans. Power Appar. Syst., Vol. PAS-104, No.2, February 1985, pp. 424-436.

[11] Edmund O. Schweitzer, III, "Evaluation and Development of Transmission Line Fault Locating Techniques Which Use Sinusoidal Steady-State Information," Proceedings of the 9th Annual Western Protective Relay Conference, Spokane, WA, October 26-28, 1982.

[12] B. Jeyasurya, and M.A. Rahman, "Accurate fault location of transmission lines using microprocessors," IEE Conference, Publication No.302, 1989, pp. 13-17.

[13] N. Kang, "Advancements in Transmission Line Fault Location," Ph.D. dissertation, Graduate School, Univ. Kentucky, Lexington, 2010.

[14] N. Hingorani, and L. Gyugyi, Understanding FACTS, Concepts and Technology of Flexible AC Transmission Systems. New Jersey: 1999, p. 209.

[15] IEEE Guide for Determining Fault Location on AC Transmission and Distribution Lines, IEEE standard C37.114-2004, June 2005.

[16] J. Mooney and G. Alexander, "Applying the SEL-321 Relay on Series-Compensated Systems," Application Guide Volume I AG2000-11, available on line at www.selinc.com.cn/detail/FileDownload.asp?FileID=594

[17] D. Goldsworthy, "A Linearized Model for MOV-Protected Series Capacitors," IEEE Transactions on Power Systems, Vol. PWRS-2, No. 4, November 1987.

[18] M. Saha, J. Izykowski, E. Rosolowski, B. Kasztenny: "A new fault locating algorithm for series compensated lines," IEEE Trans. Power Delivery, Vol. 14, No. 3, pp. 789–797, July 1999.

[19] Y. del Valle, G.K. Venayagamoorthy, S. Mohagheghi, J.-C. Hernandez, and R.G. Harley, "Particle Swarm Optimization: Basic Concepts, Variants and Applications in Power Systems," IEEE Transactions on Evolutionary Computation, vol. 12, Issue: 2, p. 171, April 2008.

[20] J. Kennedy and R. Eberhart, “Particle swarm optimization,” in Proc. IEEE Int. Conf. Neural Netw. (ICNN), Nov. 1995, vol. 4, pp. 1942–1948.

[21] R. Eberhart and J. Kennedy, “A new optimizer using particle swarm theory,” in Proc. 6th Int. Symp. Micro Machine and Human Science (MHS), Oct. 1995, pp. 39–43.

[22] M. Millonas. Swarms, Phase Transitions, and Collective Intelligence. In C.G. Langton, editor, Artificial Live III, pages 417–445. Addison-Wesley, 1994.

[23] I.N. Kassabalidis, M.A. El-Shurkawi, and R.J. Marks, “Border Identification for Power System Security Assessment using Neural Network Inversion: An Overview,” in Proceedings of the IEEE Congress on Evolutionary Computation, volume 2, pages 1075–1079. IEEE Press, May 2002.

[24] I.N. Kassabalidis, M.A. El-Shurkawi, R.J. Marks, L.S. Moulin, and A.P. Alves da Silva, “Dynamic Security Border Identification using Enhanced Particle Swarm Optimization,” IEEE Transactions on Power Systems, 17(3):723–729, August 2002.

[25] Y. Fukuyama, “State Estimation and Optimal Setting of Voltage Regulator in Distribution Systems,” in IEEE Power Engineering Society Winter Meeting, pages 930–935, 2001.

[26] Y. Fukuyama, S. Takayama, Y. Nakanishi, and H. Yoshida, “A Particle Swarm Optimization for Reactive Power and Voltage Control in Electric Power Systems,” in Proceedings of the Genetic and Evolutionary Computation Conference, pages 1523–1528, 1999.

[27] Y. Fukuyama and H. Yoshida, “A Particle Swarm Optimization for Reactive Power and Voltage Control in Electric Power Systems,” in Proceedings of the IEEE Congress on Evolutionary Computation, volume 1, pages 87–93, May 2001.

[28] H. Yoshida, Y. Fukuyama, S. Takayama, and Y. Nakanishi, “A Particle Swarm Optimization for Reactive Power and Voltage Control in Electric Power Systems Considering Voltage Security Assessment,” in Proceedings of the IEEE International

Conference on Systems, Man, and Cybernetics, volume 6, pages 497–502, October 1999.

[29] H. Yoshida, K. Kawata, Y. Fukuyama, and Y. Nakanishi, “A Particle Swarm Optimization for Reactive Power and Voltage Control Considering Voltage Stability,” in Proceedings of the International Conference on Intelligent System Application to Power System, pages 117–121, 1999.

[30] H. Yoshida, K. Kawata, Y. Fukuyama, S. Takayama, and Y. Nakanishi, “A Particle Swarm Optimization for Reactive Power and Voltage Control Considering Voltage Security Assessment,” IEEE Transactions on Power Systems, 15(4):1232–1239, November 2001.

[31] Z–L. Gaing, “Particle Swarm Optimization to Solving the Economic Dispatch Considering the Generator Constraints,” IEEE Transactions on Power Systems, 18(3):1187–1195, August 2003.

[32] S. Kannan, S.M.R. Slochanal, P. Subbaraj, and N.P. Padhy. Application of Particle Swarm Optimization Technique and its Variants to Generation Expansion Planning. Electric Power Systems Research, 70(3):203–210, 2004.

[33] P.S. Sensarma, M. Rahmani, and A. Carvalho, “A Comprehensive Method for Optimal Expansion Planning using Particle Swarm Optimization,” in Proceedings of the IEEE Power Engineering Society Transmission and Distribution conference, volume 2, pages 1317–1322, January 2002.

[34] M.A. Abido, “Optimal Power Flow using Particle Swarm Optimization,” International Journal of Electrical Power and Energy Systems, 24(7):563–571, 2002.

[35] A.I. El-Gallad, M.E. El-Hawary, A.A. Sallam, and A. Kalas, “A Swarm-Intelligently Trained Neural Network for Power Transformer Protection,” in Proceedings of the Canadian Conference on Electrical and Computer Engineering, pages 265–269, 2002.

[36] J. Kennedy and R.C. Eberhart, “Particle Swarm Optimization,” in Proceedings of the IEEE International Joint Conference on Neural Networks, pages 1942-1948. IEEE Press, 1995.

[37] R. Eberhart and Y. Shi, “Comparing inertia weights and constriction factors in particle swarm optimization,” in Proc. IEEE Congress Evol. Comput., Jul. 2000, vol. 1, pp. 84–88.

[38] R. Eberhart, Y. Shi, and J. Kennedy, Swarm Intelligence. San Mateo, CA: Morgan Kaufmann, 2001.

[39] E. Ozcan and C. Mohan, “Particle swarm optimization: Surfing the waves,” in Proc. IEEE Congress Evol. Comput., Jul. 1999, vol. 3, pp.1939–1944.

[40] R.K. Aggrwal, D.V. Coury, A.T. Johns, and A. Kalam, “Practical approach to accurate fault location on extra high voltage teed feeders,” IEEE Trans. Power Delivery, Vol.8, No. 3, July 1993, pp. 874-883.

[41] V. Cook, “Fundamental aspects of fault location algorithms used in distance protection,” IEE Proc. C, Vol. 133, No.6, 1986, pp. 354-368.

[42] A.T. Johns, P.J. Moore, and R. Whittard, “New technique for the accurate location of earth faults on transmission systems,” IEE Proc.-Gener. Transm. Distrib., Vol. 142, No. 2, March 1995, pp. 119-127.

[43] D. Tziouvaras, J. Roberts, and G. Benmouyal,” New Multi-Ended Fault Location Design for Two- or Three-Terminal Lines,” IEE Conference, Publication No.479, 2001, pp. 395-398.

[44] P. Kundur, Power System Stability and Control, EPRI, San Francisco, McGraw-Hill, 1994.

[45] A. Girgis, D. Hart, and W. Peterson, “A New Fault Location Technique for Two- and Three-Terminal Lines,” Transactions on Power Delivery, Vol. 7 No.1, January 1992

[46] A. Engelbrecht, Fundamentals of Computational Swarm Intelligence, Wiley, England, 2005.

[47] D. Novosel, D.Hart, E. Udren, and J. Garitty," Unsychronized Two-Terminal Fault Location Estimation," Transactions on Power Delivery, Vol. 1 No.1, January 1996, pp. 130-138.

BIOGRAPHICAL INFORMATION

Eithar Nashawati is Consulting Conceptual Design Engineer in System Protection at Oncor Electric Delivery Company and a Ph.D. candidate with the school of Electrical Engineering at the University of Texas at Arlington. He received his M.S.E.E. degree in Electrical Engineering from the University of Texas at Arlington in 2004. He received his B.S.E.E. degree from the University of Damascus in 1999. He worked as a Lead Protection and Control Engineer and as an Area Substation Engineer at Progress Energy Carolinas. He is a Professional Engineer in Texas and North Carolina.